Journal of Alzheimer's Disease 38 (2014) 767–786
DOI 10.3233/JAD-131091
IOS Press

Increased Efflux of Amyloid-β Peptides through the Blood-Brain Barrier by Muscarinic Acetylcholine Receptor Inhibition Reduces Pathological Phenotypes in Mouse Models of Brain Amyloidosis

Paolo Paganetti[a], Katia Antoniello[a,1], Kavi Devraj[b,1], Nicolas Toni[a,2], Dairin Kieran[a,3], Rime Madani[a], Maria Pihlgren[a], Oskar Adolfsson[a], Wolfgang Froestl[a], André Schrattenholz[c], Stefan Liebner[b], Daniel Havas[d], Manfred Windisch[d], John R. Cirrito[e], Andrea Pfeifer[a] and Andreas Muhs[a,*]
[a]*AC Immune SA, Lausanne, Switzerland*
[b]*Institute of Neurology, Medical School Goethe University, Frankfurt am Main, Germany*
[c]*ProteoSys AG, Mainz, Germany*
[d]*QPS Austria, Grambach, Austria*
[e]*Department of Neurology, Knight AD Research Center, and Hope Center for Neurological Disorders, Washington University School of Medicine, St. Louis, MO, USA*

Handling Associate Editor: Thomas Bayer

Accepted 6 August 2013

Abstract. The formation and accumulation of toxic amyloid-β peptides (Aβ) in the brain may drive the pathogenesis of Alzheimer's disease. Accordingly, disease-modifying therapies for Alzheimer's disease and related disorders could result from treatments regulating Aβ homeostasis. Examples are the inhibition of production, misfolding, and accumulation of Aβ or the enhancement of its clearance. Here we show that oral treatment with ACI-91 (Pirenzepine) dose-dependently reduced brain Aβ burden in AβPPPS1, hAβPP$_{SL}$, and AβPP/PS1 transgenic mice. A possible mechanism of action of ACI-91 may occur through selective inhibition of muscarinic acetylcholine receptors (AChR) on endothelial cells of brain microvessels and enhanced Aβ peptide clearance across the blood-brain barrier. One month treatment with ACI-91 increased the clearance of intrathecally-injected Aβ in plaque-bearing mice. ACI-91 also accelerated the clearance of brain-injected Aβ in blood and peripheral tissues by favoring its urinal excretion. A single oral dose of ACI-91 reduced the half-life of interstitial Aβ peptide in pre-plaque mhAβPP/PS1d mice. By extending our studies to an *in vitro* model, we showed that muscarinic AChR inhibition by ACI-91 and Darifenacin augmented the capacity of differentiated endothelial monolayers for active transport of Aβ peptide. Finally, ACI-91

[1]These authors contributed equally to this work.

[2]Current address: Department of Fundamental Neurosciences, University of Lausanne, Lausanne, Switzerland.

[3]Current address: Quintiles Outcome, St-Prex, Switzerland.

*Correspondence to: Dr. Andreas Muhs, CSO, AC Immune SA, EPLF Building PSE-B, CH-1015 Lausanne, Switzerland. Tel.: +41 21 693 9124; E-mail: andreas.muhs@acimmune.com.

ISSN 1387-2877/14/$27.50

was found to consistently affect, *in vitro* and *in vivo*, the expression of endothelial cell genes involved in Aβ transport across the Blood Brain Barrier (BBB). Thus increased Aβ clearance through the BBB may contribute to reduced Aβ burden and associated phenotypes. Inhibition of muscarinic AChR restricted to the periphery may present a therapeutic advantage as it avoids adverse central cholinergic effects.

Keywords: Aβ brain efflux, Aβ clearance, Aβ homeostasis, AβPP transgenic mice, amyloid-β peptides, drug treatment, muscarinic receptors, plaque deposition

INTRODUCTION

Misfolding and progressive accumulation of amyloid-β peptides (Aβ) in soluble assemblies and amyloid plaques may represent critical pathogenic factors in Alzheimer's disease (AD) [1–3]. Aβ is released from the amyloid-β protein precursor (AβPP) by endoproteolytic cleavage through β- and γ-secretase [4]. Over 160 mutations in AβPP or presenilin/γ-secretase increase the formation of toxic Aβ in familial AD [5]. AβPP transgenic mice are broadly used models of brain amyloidosis [6]. In these mice, the presence of AD-linked mutations in the transgene(s) accelerates pathology onset, exacerbates Aβ deposition, and worsens cognitive deficits, translating with fidelity the clinical findings. It is concluded that a rise in brain Aβ may drive the pathogenesis of AD. Inhibitors of Aβ production are therefore promising disease-modifying drugs tested in clinical trials [7]. However, Aβ clearance rather than production is compromised in AD [8] and targeting Aβ clearance is an emerging therapeutic approach for AD [9, 10]. Prominent examples are Aβ immunotherapies, which affect Aβ homeostasis in brain and periphery [7]. Normally, Aβ is rapidly cleared by proteolytic digestion or transport across the blood-brain barrier (BBB). Endothelial LDL receptor-related protein 1 (LRP1) regulates Aβ efflux from the brain to blood [11]. LRP1 inhibition increases brain Aβ [12–14], and LRP1 expression is reduced in AD [15]. Other transporters contribute to Aβ efflux [16] as in the case of P-glycoprotein [17]. In contrast, the receptor for advanced glycation end-products plays an important role for Aβ transport into the brain [18]. Once in the blood, Aβ is also rapidly cleared, possibly with the contribution of LRP1 [19].

AD is characterized by a loss of cholinergic neurons and muscarinic acetylcholine receptor (AChR) antagonists induce AD-like memory deficits whereas agonists promote non-amyloidogenic processing of AβPP [20, 21]. Pirenzepine is a well characterized, highly selective, negative allosteric modulator of muscarinic AChRs [22] with preference for the M1/M4 subclass [23], which was developed as an anti-ulcerative drug. In this report, we show that oral treatment with ACI-91 (Pirenzepine synthesized at AC Immune) reduces brain Aβ burden and associated phenotypes in AβPP mice. Our data suggests that the action of ACI-91 on plaque deposition may occur through an indirect mechanism initiated at the BBB. Inhibition of muscarinic AChRs on endothelial cells increases Aβ efflux from the brain to the blood and ultimately peripheral clearance into urine. Notably, this may occur without considerable central muscarinic AChR inhibition because of the poor brain penetration of ACI-91.

MATERIALS AND METHODS

Animal experimentations

This study was performed in strict compliance with the local guidelines for the care and use of laboratory animals and respecting the policies on the use of animals in neuroscience research released by the American Society of Neuroscience. Prior approval by the local ethical committees was obtained for all protocols. Surgery was performed under appropriate sedation, analgesia, or anesthesia and every effort was made to minimize distress and suffering of the animals. Group sizes were kept to the minimum required to obtain valid results.

ACI-91 testing for brain amyloid in AβPPPS1 mice

The AβPPPS1 transgenic C57BL/6J (mixed gender) mice (mThy-1 huAβPP751$_{Swe}$ × mThy-1 PS1$_{L166P}$, [24]) at four months of age were administered by gavage with 100 mg/Kg ACI-91 ($n = 12$) or vehicle (2 × PBS, $n = 11$) as a 10 mL/Kg solution for 33 days. Six hours after the last dosing, mice were killed by lethal narcosis with Ketamine/Rompun and brains collected after intracardial perfusion with 0.9% NaCl.

The right hemisphere was fixed in 4% PFA in PBS for 16 h. Thirty consecutive 40 μm coronal vibratome

sections (lateral between 2.18 and 1.08 mm in the region of the subiculum) were stored at 4°C in PBS with 0.1% sodium azide. Free floating sections 1, 7, 13, 19, 25 were incubated in Nett-wells to stain all sections in one single assay and minimize intensity variation. Sections were washed twice in PBS and incubated for 15 min in 1.5% hydrogen peroxide in PBS and methanol (1:1) to remove endogenous peroxidase activity. After three washes in PBS with 0.1% Triton X100 (PBST), the sections were blocked for 30 min in 10% FCS in PBST followed by an overnight incubation with a biotinylated antibody against the N-terminus of Aβ (reMYND). The signal was detected with an avidin-biotin peroxidase complex (Vectastain ABC, Vector) and 3,3′-diaminobenzidine tetrahydrochloride (ICN, 1 tablet/10mL Tris with 3 μl hydrogen peroxide). Sections were dehydrated once in ethanol and xylene and mounted in Depex (BDH Laboratory).

ACI-91 testing for brain amyloid and Aβ peptides in hAβPP$_{SL}$ mice

Two studies were conducted with female hAβPP$_{SL}$ C57BL/6xDBA mice (mThy-1 huAβPP751$_{Swe\&London}$, [25]). In the first study, mice at the age of 6.5 ± 0.5 months were administered by gavage with 5 mg/Kg ($n = 19$) or 100 mg/Kg ($n = 17$) ACI-91 or vehicle (2xPBS, $n = 14$) for 33 days. In the second study, mice at the age of 7.0 ± 0.5 months were administered by gavage with 5 or 20 mg/Kg ACI-91 (both groups $n = 21$) or vehicle (20 mM PB pH 7.4, $n = 14$) for 33 days. Age-matched non-transgenic littermates ($n = 15$) received the same treatment with vehicle. Six hours after the last oral application all mice were sedated with Isofluran (Baxter). Cerebrospinal fluid (CSF) was obtained by suctioning and capillary action using a pipette inserted to the depth of 0.3–1 mm into the foramen magnum. Blood from the right cardiac ventricular chamber was collected into EDTA vials to obtain plasma after centrifugation at 700 *g* for 10 min.

For both studies, after extensive perfusion with PBS, brains were then rapidly dissected in two hemispheres without the cerebellum. The right forebrain hemispheres were fixed in 4% PFA in PBS for 1 h and transferred to a 15% sucrose PBS solution for 24 h to ensure cryoprotection for freezing in liquid isopentane before storage at −80°C. A systematic random set of five 10 μm cryosections deriving from five different medio-sagittal levels were processed for plaque load ($n = 8$ for each group, randomly selected). Immune reactivity was quantitatively evaluated in the hippocampus and in the cortex using the human Aβ-specific antibody 6E10 (Signet) and fluorescent Cy3-labeled secondary antibody (Jackson Immuno Research). Tiled images were recorded using a Nikon DS-Qi1MC camera mounted on a Nikon E800 microscope together with an automatic controlled table (StagePro). Plaque pathology was analyzed for the number and area of 6E10 positive plaques (minimal size of 150 μm^2).

The left forebrain hemispheres were frozen in liquid nitrogen and stored at −80°C for biochemical analysis. The tissue was homogenized [26] in 5 mL TBS (20 mM Tris, 137 mM NaCl, pH 7.6, protease inhibitor cocktail), centrifuged (74200 *g* for 1 h at 4°C) and the resulting supernatant stored at −20°C as TBS fraction. The pellet was resuspended in 2.5 mL 1% Triton X100 in TBS, centrifuged as above and the supernatant stored at −20°C as Triton X100 fraction. These steps were repeated sequentially with 2.5 mL 2% SDS in water (SDS fraction) and with 0.5 mL 70% formic acid in water (neutralized with 9.5 mL 1 M Tris, FA fraction). All samples were used for $A\beta_{x\text{-}40}$ and $A\beta_{x\text{-}42}$ determination by ELISA (The Genetics Company, Switzerland). It is assumed that soluble monomeric to oligomeric Aβ are contained in the TBS and Triton X100 fractions, whereas protofibrils and water insoluble fibrils are dissolved in SDS and formic acid.

For the analysis of cerebral amyloid angiopathy, 10 μm cryosections from three medio-sagittal brain levels of six perfused hAβPP$_{SL}$ mice were double stained using 6E10 for the Aβ deposits and with an anti-alpha smooth muscle actin (SMA) antibody (Abcam) and Cy5-secondary antibody (Jackson Immuno Research). Deposited Aβ immune reactivity was determined within cross-sections of meningeal neocortical SMA positive vessels at 11 different positions per section.

Behavioral testing with hAβPP$_{SL}$ mice

All animals had dark eyes and were likely to perceive the landmarks outside the water maze pool. However, visual abilities were assessed in the visible platform pretest training (two 1 min trials) before treatment started and one-day before start of the water maze test. Only animals that fulfilled this task were used for the study. The water maze task was conducted in a black circular pool with a diameter of 100 cm containing a transparent platform 8 cm in diameter placed about 0.5 cm beneath the water surface in the southwest quadrant of the pool. Task learning was performed on four consecutive days (three 1 min trials). If a mouse

did not find the platform within 1 min, it was manually placed on the platform. Task learning was monitored with a computerized tracking system (Biobserve) for escape latency (time needed to find the platform), pathway (trajectory length), and speed. The probe trial was done 1 h after the last learning trial on day 4 with the platform removed from the pool. Measurements in the goal quadrant included abidance (absolute and percent time) and pathway were measured during 30 seconds.

Analysis of Aβ efflux and plaques in AβPP/PS1 mice

Female AβPP/PS1 (mThy-1 $hA\beta PP_{V717I}$ × hThy-1 $PS1_{A246E}$, [27]) mice at 11 months of age were administered by gavage with 20 mg/Kg ACI-91 or vehicle (20 mM PB pH 7.4) for 33 days (both groups $n = 12$). Two hours after the last administration, mice were anesthetized with Isofluran and treated s.c. with 0.1 mg/Kg Buprenorphine before starting surgery. In the stereotaxic frame, a hole was drilled into the cranium at coordinates anterior 0.5 mm and lateral ± 2.0 mm from Bregma. A silica fiber mounted on a 30 G canula was placed 3.5 mm from dura mater and 7.5 pmoles (0.5 μL) biotin-$A\beta_{1\text{-}40}$ (Anaspec) dissolved in 148 mM NaCl, 3 mM KCl, 1.4 mM $CaCl_2$, 0.75 mM $MgCl_2$, 0.8 mM Na_2HPO_4, and 0.2 mM NaH_2PO_4 were injected over 1 min with a 10 μL Hamilton syringe. The canula was carefully removed after 5 min and mice were killed 15, 30, or 45 min later (each group $n = 4$). Brain hemispheres were dissected, weighed, and stored frozen at −80°C.

The injected hemispheres were homogenized in 5 volumes of 250 mM sucrose, 1 mM EDTA, 1 mM EGTA, 20 mM Tris/Cl pH 7.4, protease inhibitors (Millipore) using a glass Dounce homogenizer. After adding an equal volume of 0.4% diethylamine hydrochloride, homogenates were centrifuged (64000 *g* for 1 h at 4°C; Optima L-80XP Beckman Coulter) and supernatants neutralized with 10% of the final volume using 0.5 M Tris/Cl pH 6.8 (DEA fraction). For biotin-$A\beta_{1\text{-}40}$ determination, the peptide was enriched and the brain tissue was removed from the matrix using CaptAvidin agarose (Invitrogen) resuspended in 10.8 mM Na_2HPO_4 and 44.6 mM citrate, pH 2.6. Ten μL of the 1:1 (V/V) agarose slurry was added to 250 μL DEA fraction and incubated on a rotator for 30 min at room temperature. Beads were centrifuged (3000 *g* for 15 min at 4°C) and washed once with 1 mL of 10 mM Tris/Cl pH 7.0. Biotin-$A\beta_{1\text{-}40}$ was eluted in 20 μL of 50 mM Na_2CO_3, pH 10 by gentle shaking for 30 min at room temperature. To determine $A\beta_{1\text{-}40}$ using an AlphaLISA assay, 10 μL of the eluate were used mixed with 12.5 ng/mL 6E10 (final concentration), 20 μg/mL acceptor beads coupled to anti-mouse IgG (PerkinElmer), and 40 μg/mL streptavidin-donor beads (PerkinElmer) in 50 μL final volume and the signal measured with an EnSpire Alpha 2390 Reader (PerkinElmer).

Ten 10 μm sagittal cryosections were cut from contralateral hemibrains starting ∼3.54 mm lateral from midline resulting in five consecutive sections from 12 medio-lateral levels. Plaque pathology was analyzed for number and area as well as the mean intensity of 6E10 positive plaques stained as described above using random sections at levels 2, 4, 6, 8, and 11 (both groups $n = 12$). For Thioflavin S staining, air-dried cryosections where washed in PBS for 5 min, incubated for 15 min in 0.5% Thioflavin S protected from light, washed for 3 min with 80% ethanol and twice with for 5 min with PBS, and mounted with Moviol and coverslips ($n = 6$, randomly selected).

Analysis of Aβ efflux in $hA\beta PP_{SL}$ mice

Female $hA\beta PP_{SL}$ mice at an age of 9 months were administered 20 mg/Kg ACI-91 or vehicle (20 mM PB pH 7.4) for 33 days (first study, both groups $n = 9$) or 37 days (second study, both 20 min groups $n = 7$, both 40 min groups $n = 9$). Two hours after the last compound application, animals were preemptively treated for analgesia via s.c. injection with 5 mg/Kg Carprofen and anesthetized with a mixture of Ketasol/Xylazin. In the first study, 0.07 pmoles [^{125}I]$A\beta_{1\text{-}40}$ in 1 μL (70 nM) were intracerebrally injected into the striatum (0.5 mm anterior and ± 2.0 mm lateral from Bregma, 3.5 mm deep from dura mater) using a Hamilton syringe (1.0 μL volume, outer needle diameter 0.48 mm, inner diameter 0.13 mm, blunt end) at a flow-rate of 0.5 μL/min. The activity of [^{125}I]$A\beta_{1\text{-}40}$ used for injection was 4800 Bq/μL ($\eta = 75\%$, 216 000 cpm/μL), the monoiodinated peptide was purified by HPLC, analyzed by MALDI MS and applied in 1 μL artificial interstitial fluid (ISF) (148 mM NaCl, 3 mM KCl, 1.4 mM $CaCl_2$, 0.75 mM $MgCl_2$, 0.8 mM Na_2HPO_4, 0.2 mM NaH_2PO_4). In the second study, animals were intracerebrally injected with 0.11 pmoles of [^{125}I]$A\beta_{1\text{-}40}$ and 83 μg [^{14}C]inulin at a radioactivity ratio 2:1 (7400 and 3700 Bq, respectively). Mock-injected nontransgenic littermates at the same age were used for baseline radioactivity measurements. In the first study, the canula was carefully removed 5 min after intrathecal injection and 15 min later CSF, heparinized blood,

hemisected brain, liver, and kidney were collected for radioactivity measurement by liquid scintillation. In the second study, the needle was removed 9 min after intrathecal injection and 11 min (20 min time point) or 31 min (time point 40 min) later, animals were sacrificed and blood, hemisected brain, stomach, and urine were collected. For urine collection, the urethral orifice was pasted with VetGlu® to avoid urination during anesthesia and urine collected at sacrifice. The quantity of [^{125}I]A$\beta_{1\text{-}40}$ and [^{14}C]inulin was measured in the different tissues by liquid scintillation counting. In a further study, 8 month-old non-transgenic female littermates received an intracerebral injection of 0.19 pmoles [^{125}I]A$\beta_{1\text{-}40}$ (12500 Bq) and were killed 20 and 60 min later. CSF, blood, hemisected brain, heart, lung, liver, intestine, kidney, and urine were collected for the determination of [^{125}I]A$\beta_{1\text{-}40}$ radioactivity. Biodistribution of [^{125}I]-labeled ligand was calculated as published [28, 29].

In vivo microdialysis

Female mhAβPP/PS1d (mPrion mo/huAβPP695swe × mPrion PS1dE9, [30]) mice at 3 months of age were implanted unilaterally with a microdialysis guide canula (Bioanalytical Systems) into the hippocampus at stereotaxic coordinates Bregma −3.1 mm, midline −2.5 mm, and 1.2 mm below dura mater [31, 32]. 38-kDa molecular weight cut-off microdialysis probes (BR-style, Bioanalytical Systems) that were 2 mm in length were inserted through the canula so the probe was contained entirely within the hippocampus. Animals recovered for 6–8 h and then ISF was sampled hourly for 6 h to determine baseline Aβ levels in each mouse. Microdialysis probes were perfused with artificial CSF [31] containing 4% bovine serum albumin at a constant flow-rate of 1 μl/min. After baseline collection, mice were administered vehicle (sterile 20 mM PB pH 7.4, $n = 9$) or 20 mg/Kg ACI-91 ($n = 10$) by oral gavage and ISF Aβ sampled every 60 min for 24 hr. One day after initial dosing, animals were re-administered either vehicle ($n = 6$) or 20 mg/Kg ACI-91 p.o ($n = 7$), 4 h later, when ACI-91 effect on ISF Aβ started, mice were injected with a potent γ-secretase inhibitor, 30 mg/Kg i.p. Compound E [33] to rapidly block Aβ generation [34]. ISF Aβ was measured for an additional 4 h after Compound E-treatment. During sample collection, ISF samples were stored in a refrigerated fraction collector. All microdialysis samples were assessed for A$\beta_{x\text{-}40}$ by sandwich ELISA immediately following each experiment. At experiment conclusion, the brains were removed and fixed overnight in 4% PFA then processed for histological verification of probe placement.

Determination of ACI-91 concentration in tissues

About 200 mg brain samples were homogenized in 5 mL TBS 137 mM NaCl, 20 mM Tris, pH 7.6 and cocktail of protease inhibitors. Then, 100 μL of the brain homogenate was diluted with 500 μL water and centrifuged for 5 min at 3000 *g*. 500 μl of the supernatant was used for solid phase extraction and resuspended in 10% acetonitrile in water. Ten μL CSF was mixed with 30 μl 10% acetonitrile in water, whereas plasma was analyzed directly. All samples were then injected into the UPLC-MS/MS for compound determination using clozapine as internal standard. The compound determination was performed at Quality Assistance SA (Donstiennes, Belgium).

Isolation of MBMECs and MBMVs

Primary mouse brain microvascular endothelial cells (MBMECs) were isolated from 8–10 adult BL6/C57 mice in each preparation as described previously with only modification being the use of a dounce homogenizer instead of mincing the tissue [35]. Cultures were maintained and routinely characterized for endothelial markers such as claudin-5, VE-cadherin, and PECAM by immune fluorescence as described previously [35]. For RNA isolation, mouse brain microvessels (MBMVs) were isolated from female hAβPP$_{SL}$ mice at an age of 10 months that were administered 20 mg/Kg ACI-91 or vehicle (20 mM PB pH 7.4) for 33 days. A shortened procedure to assure good RNA quality was used as described previously [36] and included the use of a single 70-micron mesh from which microvessels were collected leaving out the washing step with glass beads.

In vitro Aβ transport assay

MBMECs at three days after isolation were seeded onto 24-well transwell inserts (1.0 micron polyethylene terephthalate, GreinerBio) at 100,000 cells/cm^2. Three days later after reaching confluency, the MBMEC monolayers were treated with 10 μM ACI-91 for 24 h. As a measure of monolayer integrity, impedance measurements were performed to obtain the transendothelial electrical resistance (TEER) as described previously [37]. To continuously measure TEER, plates were transferred after seeding to a

cellZscope® device (Nanoanalytics, Germany). Compound effect on TEER was analyzed for MBMEC monolayers treated with 140 μM ACI-91 for 24 h, TEER values for triplicate inserts were obtained with vehicle control set to 100%. To start the Aβ transport assay, cells were washed once with PBS before adding 1 μM diethylaminocoumarin $A\beta_{1\text{-}40}$ (DEAC-Aβ, Anaspec) and 5 μM Texas red 3 kDa dextran (TxR-3kDa dextran, Invitrogen) dissolved in 200 μL PBS to the top chamber and plain 1000 μL PBS to the bottom chamber. Aliquots (20 μL from the top chamber and 100 μL from the bottom chamber) were collected at 10 min of incubation. The samples from the top chamber were then diluted to 100 μL with PBS. These aliquots keep the ratio of top chamber volume to bottom chamber at the same level, which is important to eliminate hydrostatic pressure effects. Fluorescent analytes were determined using a fluorescence plate reader (Infinite 200, TECAN) with excitation and emission set at 595/625 for TxR and 426/462 nm for DEAC. In all the experiments, a single data point represents the relative fluorescence unit (RFU) ratio of bottom over top chamber of a single transwell insert. One of the control wells was set to 100% in each experiment and all values were divided by the population mean from all control experiments to establish an overall normalization without affecting the standard error. Similar experimental setup was also utilized for an alternate *in vitro* model using bEnd5 cells, an immortalized mouse brain endothelioma cell line characterized as an *in vitro* BBB model [38]. Darifenacin was obtained from a commercial source (Santa Cruz Biotechnology).

qPCR analysis

Total RNA was isolated using Qiagen RNEasy mini kit following the manufacturer's protocol followed by cDNA preparation using Reverse transcriptase kit. The protocols for qPCR run and analysis were exactly as described previously [39].

Statistics

Average and SEM were calculated for all measured parameters. Outliers within a group were detected by Grubbs test and were excluded from all calculations. Graphpad Prism 5.0 was utilized for statistics (as specified in the figure legends) and for preparing the graphs. Pearson test was used to analyze the correlation between measurements. For the behavioral data, all measurement were analyzed by D'Agostino & Pearson omnibus normality test, then analyzed by two-way ANOVA repeated measurements (learning sessions) or one-way ANOVA (probe trial) followed by Bonferroni multiple comparison *post hoc* analysis.

RESULTS

ACI-91 reduces plaque pathology in AβPPS1 and $hA\beta PP_{SL}$ mice

In AβPPPS1 transgenic mice, neocortical plaque deposition starts at one month of age and progressively leads to considerable brain amyloidosis, with an increase of about 34% between the fourth and fifth months of age [24]. A therapeutic protocol was designed to treat AβPPPS1 transgenic mice starting at the fourth month of age and lasting for one month with a daily oral dose of 100 mg/Kg ACI-91 or vehicle. Over the whole treatment period, no adverse effects on general behavior or body weight of the mice were observed (not shown). Six hours after the last treatment, brains were collected and processed for immune histochemical analysis of plaques using a human Aβ antibody (Fig. 1A). The vehicle-treated control mice presented a plaque burden covering $2.44 \pm 0.14\%$ of the neocortical area (Fig. 1B) in agreement with published data [24]. ACI-91-treatment significantly reduced plaque deposition by 27% to a value corresponding to $1.77 \pm 0.14\%$ of the neocortical area. Considering the 34% increase in plaque load reported for the period between four and five months of age, ACI-91 may have thus reduced the plaque deposition rate by 60–80% in the neocortex of AβPPPS1 mice. No biochemical analysis for soluble or insoluble Aβ was performed in this study.

A similar treatment protocol was then applied to a transgenic mouse model solely based on mutated AβPP expression, the $hA\beta PP_{SL}$ mice, which display plaque onset at about 3 months of age [25]. In these mice, two independent experiments were performed. In the first study, two doses of ACI-91 corresponding to 5 and 100 mg/Kg or vehicle (2x PBS) were given daily by gavage for 33 days starting at an age of 6.5 months. In the second experiment, the ACI-91 doses were 5 and 20 mg/Kg or vehicle (20 mM PB pH 7.4) and the treatment started at 7.0 months of age. Also in this mouse model, ACI-91 was well tolerated. Wet weight of hemispheres as well as cortical and hippocampal area measured in sectioned tissue were highly constant for all brains investigated, indicating no treatment-induced brain atrophy (not shown). In the first experiment, histological brain examination (Fig. 2A) revealed an ACI-91 dose-dependent

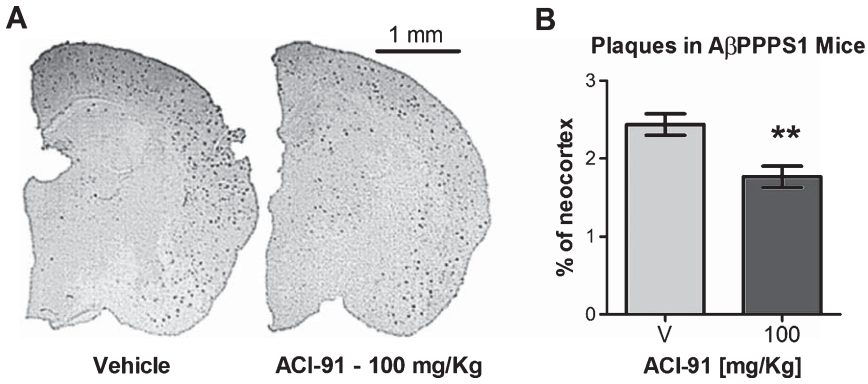

Fig. 1. ACI-91 reduces plaque pathology in AβPPPS1 transgenic mice. Four month-old AβPPPS1 mice were treated for 33 days by gavage with vehicle ($n = 11$) or 100 mg/Kg ACI-91 ($n = 12$) and analyzed for plaque pathology. A) Representative micrographs of hemibrain cross sections stained with an anti-Aβ antibody and secondary antibody coupled to horseradish peroxidase. B) Quantification of Aβ-immune stained plaque area as percent of total neocortical area. Values are shown as average ± SEM. $^{**}p = 0.002$, two-tailed unpaired student t-test.

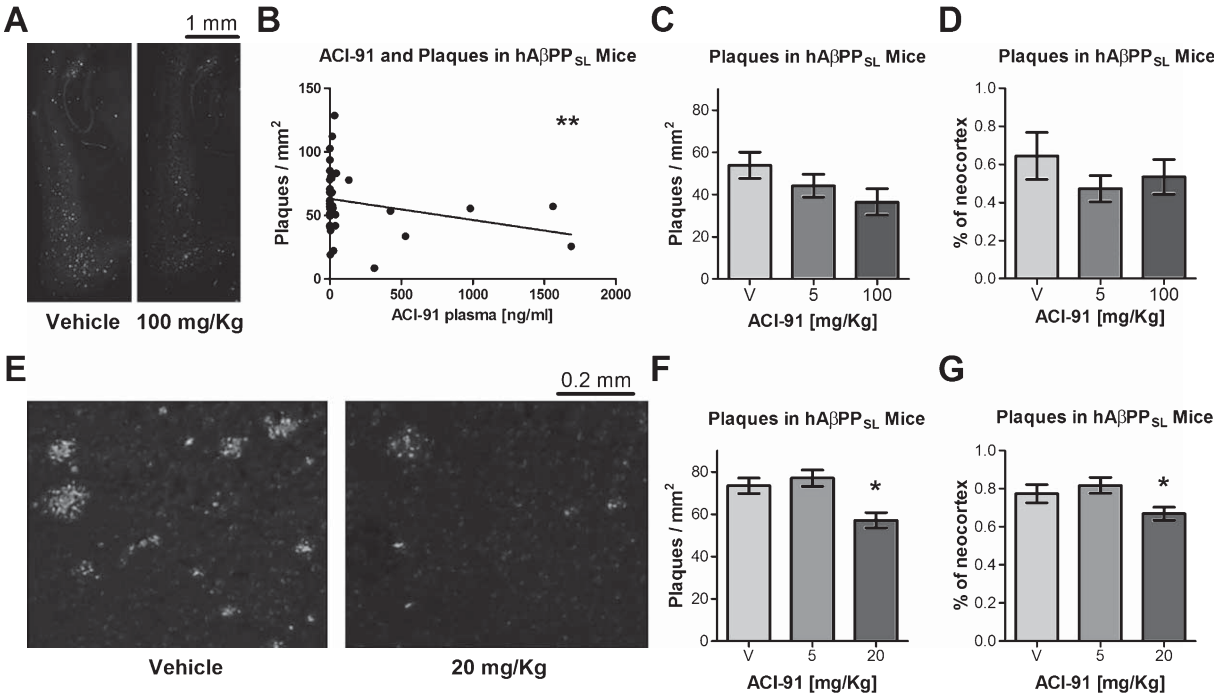

Fig. 2. ACI-91 reduces plaque pathology in hAβPP$_{SL}$ transgenic mice. A-D) hAβPP$_{SL}$ mice at 6.5 months of age were treated orally for 33 days with vehicle or 100 mg/Kg ACI-91 ($n = 8$). A) Representative micrographs of hippocampal/neocortical cryosections stained with an anti-Aβ antibody and a fluorescent secondary antibody. B) For the drug treatment animals, regression analysis reveals an inverse correlation between ACI-91 concentration in plasma and plaque density (Pearson $r = -0.54$, $^{**}p = 0.009$). Quantification of Aβ-positive plaque density (C) and Aβ-positive plaque area as percent of neocortical area analyzed (D). E-G) In a second experiment, hAβPP$_{SL}$ mice at 7 months of age were treated orally for 33 days with vehicle, 5 or 20 mg/Kg ACI-91 ($n = 8$). E) Representative micrographs of neocortical regions stained with an anti-Aβ antibody and a fluorescent secondary antibody. Compound treatment led to a dose-dependent reduction in Aβ plaque number (F) and area (G). $^{*}p < 0.05$ by one-way ANOVA and Dunnett's multiple comparison test to vehicle. Values in C, D, F, and G are shown as average ± SEM.

reduction of plaque number that negatively correlated with the amount of ACI-91 (Fig. 2B), although mean cohort analysis did not reach statistical significance (Fig. 2C) also for the neocortical plaque area (Fig. 2D). In the second experiment, histological brain examination (Fig. 2E) showed that treatment with 20 mg/Kg ACI-91, but not with 5 mg/Kg ACI-91, led to a significant, although moderate, decrease of neocortical plaque number by 22% (Fig. 2F) and plaque area by 14% (Fig. 2G). In both hAβPP$_{SL}$ mice experiments,

Table 1
Non-parametric Spearman's correlations between brain ACI-91 and Aβ in the SDS or formic acid (FA) fractions (32 pairs), brain ACI-91 and Aβ in cortical spinal fluid (CSF; 30 pairs) or plasma ACI-91 and plasma Aβ (71 pairs)

	$A\beta_{x-40}$				$A\beta_{x-42}$			
	SDS	FA	CSF	Plasma	SDS	FA	CSF	Plasma
Spearman R	−0.35	−0.53	−0.61	0.26	−0.63	−0.52	−0.70	0.27
Two-tailed p	0.053	0.0017	0.0004	0.028	0.0001	0.0021	<0.0001	0.024

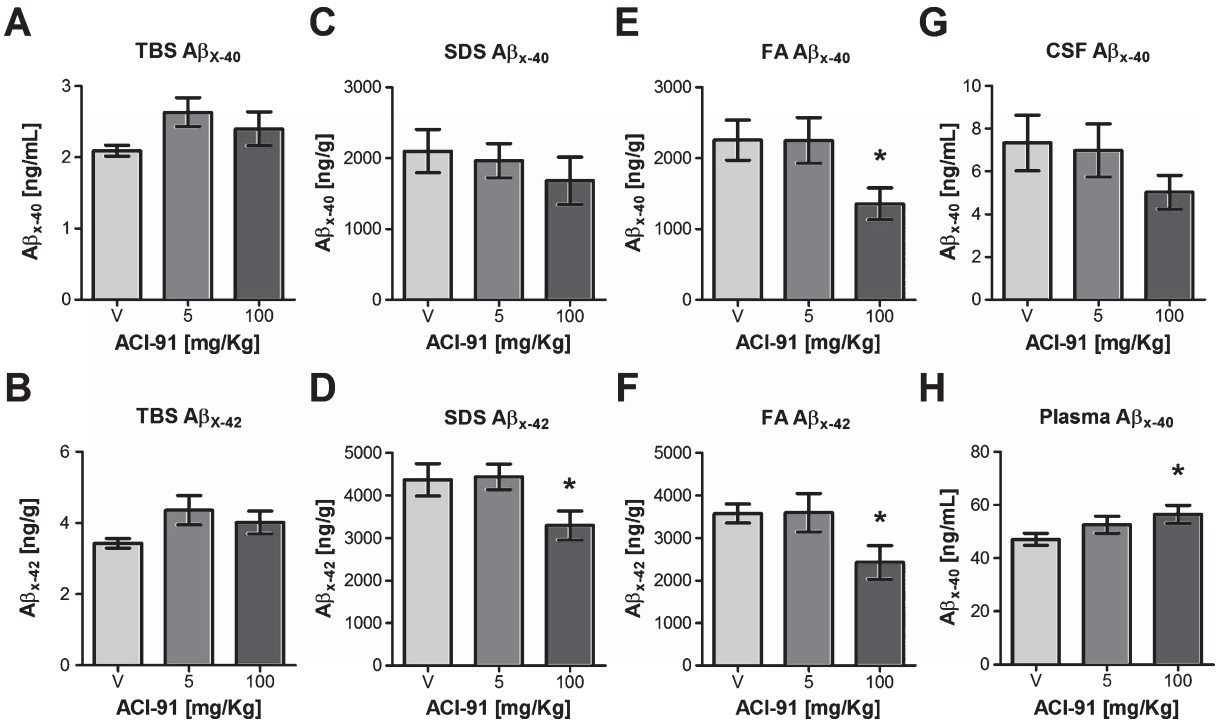

Fig. 3. Reduced brain Aβ load and increased plasma Aβ by oral administration with ACI-91. 6.5 month-old $hA\beta PP_{SL}$ mice were treated orally for 33 days with vehicle (V, $n = 13$-14) or the indicated doses of ACI-91 ($n = 14$–20). Brain homogenates were and analyzed with human $A\beta_{x-40}$ and $A\beta_{x-42}$ specific ELISA after extraction with increasing stringent conditions: water (TBS) soluble (A, B), SDS soluble (C, D), formic acid (FA) soluble (E, D; $^*p < 0.05$ by one-way ANOVA and Dunnett's multiple comparison test to vehicle. F; $^*p < 0.05$ by two-tailed unpaired student *t*-test). $A\beta_{x-40}$ was also determined in CSF (G) and plasma (H; *by two-tailed unpaired student *t*-test). All values are shown as average ± SEM.

the hippocampus of mice displayed at the end of these studies a relatively low plaque load and no compound-related effect was determinable (not shown).

ACI-91 reduces insoluble Aβ in hAβPP$_{SL}$ mice

The brains of the $hA\beta PP_{SL}$ mice were also biochemically processed to determine the amount of $A\beta_{x-40}$ and $A\beta_{x-42}$ peptides using an extraction protocol with increasingly stringent conditions. Consistent with the histological data showing reduced plaque load, a negative correlation was observed between ACI-91 levels and insoluble Aβ in the brain fractions extracted with SDS or formic acid (Table 1). Mean cohort analysis revealed that no changes were found for soluble $A\beta_{x-40/42}$ (Fig. 3A, B), whereas 100 mg/Kg ACI-91 reduced the amount of aggregated, water-insoluble $A\beta_{x-40/42}$ peptides extracted by SDS (Fig. 3C, D) and formic acid (Fig. 3E, F), but only the latter reached significance. In modified AβPP transgenic mouse models with strong $A\beta_{42}$ production as for AβPP carrying the Swedish and London mutations used in this study, a SDS-resistant, formic acid-extracted Aβ population is found as previously described for other models [40]. Moreover, ACI-91 brain levels correlated significantly with reduced CSF $A\beta_{x-40/42}$ and increased plasma $A\beta_{x-40/42}$ (Table 1), although cohort analysis revealed a significant effect for $A\beta_{x-40}$ only in plasma (Fig. 3E, F). Following the 33 day-treatment at 100 mg/Kg, the amount of ACI-91

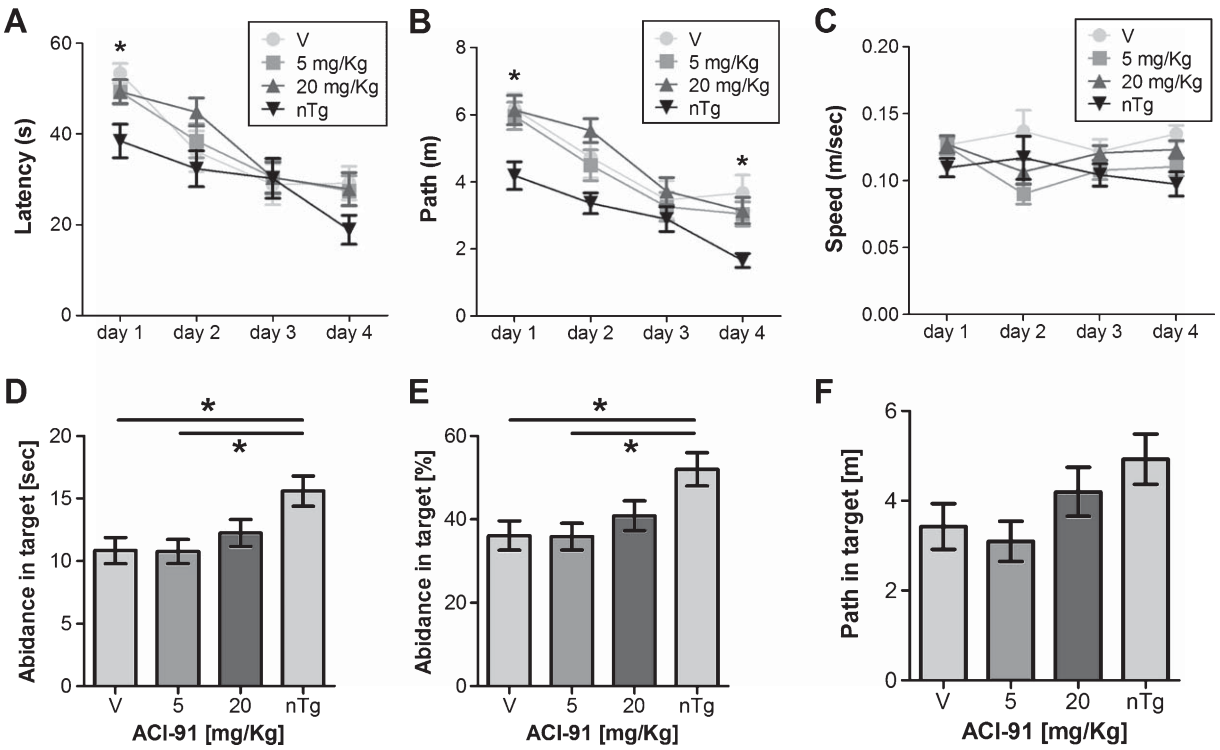

Fig. 4. ACI-91-treatment improves behavioral deficits. A) Seven month-old hAβPP$_{SL}$ mice were treated orally for 33 days with vehicle (V) or 5 or 20 mg/Kg ACI-91 and subjected to a water maze test. Age-matched non-transgenic littermates treated with vehicle (nTg) were used as control. In the learning sessions (three learning trials on four consecutive days) escape latency to reach the visible platform (A), path length (B), or speed (C) were measured (*$p < 0.05$ for the vehicle-treated transgenic versus non-transgenic mice by two-way ANOVA repeated measures followed by Bonferroni *post hoc* analysis). In the probe trial after removal of the platform, vehicle-treated ($n = 14$) and 5 mg/Kg-treated ($n = 21$) mice spent less absolute (D) and relative (E) time in the target quadrant that contained the escape platform during the training sessions when compared to vehicle-treated non-transgenic siblings ($n = 15$). In contrast, animals treated with 20 mg/Kg ($n = 21$) did not behave statistically different from the non-transgenic animals (*$p < 0.05$, one-way ANOVA). No effects were found for path length (F). Values are shown as average ± SEM.

detected in brain was 3.05 ± 0.53 ng/g (mean ± SEM, $n = 32$), which corresponded to ∼2% of the plasma levels (141.6 ± 39.6 ng/mL, $n = 73$), consistent with the poor brain penetration reported for ACI-91 [41]. As observed for the plaque analysis (Fig. 2), Aβ peptides measured in all extraction fractions obtained from mice treated with 5 mg/Kg ACI-91 were unchanged when compared to the vehicle control treated mice (Fig. 3).

ACI-91 restores behavioral deficits and brain microvessel pathology in hAβPP$_{SL}$ mice

In the second experiment, the hAβPP$_{SL}$ mice were subjected to a water maze test together with their non-transgenic littermates just before termination of the study.

The water maze test revealed during the learning sessions (three learning trials on four consecutive days; two-way ANOVA repeated measurements) no difference between the groups for escape latency or speed (Fig. 4A, C). For path, a significant time effect ($p < 0.0001$) and group effect ($p < 0.0019$), but not significant interaction (Fig. 4B), was found. Bonferroni *post hoc* analysis showed that for the vehicle-treated transgenic group a longer path was measured at day 1 and day 4 in comparison to the non-transgenic group ($p < 0.05$). Only in the beginning of the test, treated group with 5 mg/Kg (day 1, $p < 0.05$) and 20 mg/Kg (day 1 and 2, $p < 0.01$) ACI-91 were significantly different from the non-transgenic mice. This indicated that at the end of the learning session, the observed difference between transgenic and non-transgenic mice was not observed for the ACI-91 treated groups. More importantly, the probe trial performed at the end of day 4 after removing the platform revealed that hAβPP$_{SL}$ mice spent significantly less time in the target quadrant (absolute and percent; $p < 0.05$; Fig. 4D, E) than their non-transgenic littermates. Compound treatment effects were rather moderate since no improved learning ability as compared to vehicle-

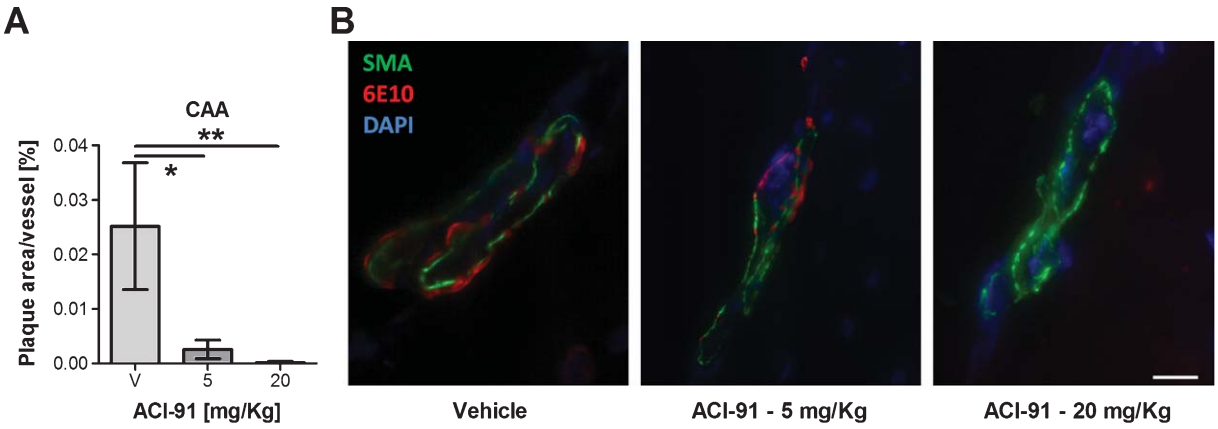

Fig. 5. ACI-91-treatment improves microvessel pathology. A) Shown is the number of smooth muscle actin-positive vessels stained for amyloid with the 6E10 Aβ-antibody. Values are shown as average ± SEM. *$p < 0.05$ and **$p < 0.01$, one-way ANOVA and Dunnett's multiple comparison test to vehicle control. B) Fluorescent micrographs of representative brain microvessels from mice treated with vehicle, 5 mg/Kg ACI-91, or 20 mg/Kg ACI-91 and stained for smooth muscle actin (SMA, green), cerebral amyloid angiopathy with an Aβ antibody (6E10, red), and nuclei (DAPI, blue). Scale = 10 μm.

treated transgenic mice was observed. Nevertheless, $hA\beta PP_{SL}$ mice treated with 20 mg/Kg ACI-91, but not with 5 mg/Kg ACI-91, did not differ significantly from their non-transgenic littermates thus effectively reversing the learning disability observed in the transgenic mice (Fig. 4D, E) No effects were observed for path in the probe trial (Fig. 4F).

At the end of the study, the $hA\beta PP_{SL}$ mice showed a moderate amyloidosis covering ∼0.025% of the mean meningeal vessel diameter (cerebral amyloid angiopathy). Treatment with both doses of ACI-91 reduced the amount of amyloid detected in SMA-positive vessels (Fig. 5A, B). Importantly, we did not find any evidence for increased brain microhemorrhages by Prussian blue staining in hippocampus and neocortex of ACI-91 treated animals (not shown).

ACI-91 reduces plaque deposition and increases Aβ brain efflux in AβPP/PS1 mice

Based on the low brain concentration reached after oral administration of ACI-91, we then investigated whether reduced Aβ accumulation in brain was caused by increased Aβ efflux through the BBB. To this end, AβPP/PS1 mice at 11 months of age were subjected to the same study protocol used in the previous studies, i.e., ACI-91 treatment for 33 days by daily gavage. Then, two hours after the last compound or vehicle administration, 7.5 pmoles biotinylated human $A\beta_{1\text{-}40}$ were injected into the striatum. Brains were collected 15, 30, and 45 min after Aβ injection and hemisected. The intrathecally injected brain hemispheres were analyzed for residual biotin-$A\beta_{1\text{-}40}$, whereas the contralateral hemispheres were analyzed for plaque burden. In the vehicle-treated mice, rapid clearance of biotin-$A\beta_{1\text{-}40}$ was completed within the first 30 min after injection as no significant difference between 30 and 45 min was found (Fig. 6A). At 15 min post-injection, in the ACI-91-treated mice the amount of biotin-$A\beta_{1\text{-}40}$ recovered from the brain was reduced by 28% when compared to the vehicle-treated mice (Fig. 6B). Histological examination of the contralateral hemibrains with a human Aβ antibody revealed a medio-lateral gradient of plaque staining intensity, which was reduced in the ACI-91 mice in the two investigated regions, neocortex (Fig. 6C, F) and hippocampus (Fig. 6D, G). In the AβPP/PS1 mice, plaque area and number were not affected significantly when comparing the two treatment groups, suggesting that the more rapid Aβ clearance found for the ACI-91 mice may result from decreased recruitment of soluble Aβ into preexisting plaques rather than from a general effect on plaque deposition. Consistent with this notion, we found a decrease in Thioflavin S positive plaques in the ACI-91-treated mice (Fig. 6E), suggesting hindered plaque maturation.

ACI-91 increases brain clearance of Aβ in $hA\beta PP_{SL}$ and mhAβPP/PS1d mice

In order to study Aβ efflux more accurately, we then analyzed [^{125}I]$A\beta_{1\text{-}40}$ clearance [42] in brain and periphery of nine month-old $hA\beta PP_{SL}$ mice treated for 33 days with 20 mg/Kg ACI-91. For this, [^{125}I]$A\beta_{1\text{-}40}$

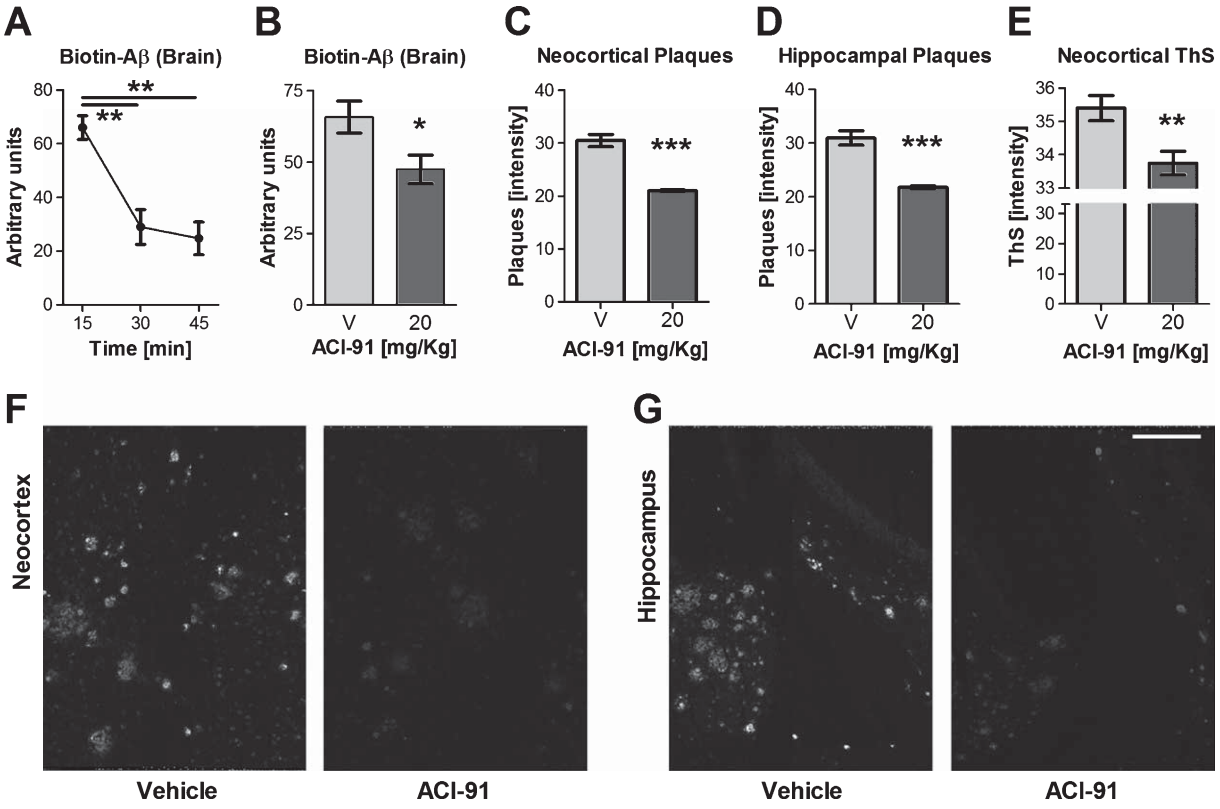

Fig. 6. ACI-91 increases Aβ brain clearance and reduces Aβ plaque pathology. Eleven month-old AβPP/PS1 mice were administered for 33 days by gavage with vehicle or 20 mg/Kg ACI-91. A) Two hours after the last administration, animals were intrathecally injected in the striatum with 7.5 pmoles/0.5μL biotin-$A\beta_{1\text{-}40}$ and for the vehicle group the injected brain hemispheres were analyzed for residual biotin-Aβ at different time points ($n=4$; $^{**}p<0.01$ by one-way ANOVA and Bonferroni's multiple comparison test, no significant difference between 30 and 45 min). B) Shown is the effect of ACI-91 treatment on residual brain biotin-Aβ at 15 min after the injection ($n=4$). C, D) The contralateral hemispheres were histologically analyzed for Aβ-positive plaques in the neocortex or hippocampus ($n=12$). E) Neocortical sections were also analyzed for Thioflavin S (ThS)-positive plaques ($n=6$). All values are shown as average ± SEM. $^{*}p<0.05$, $^{**}p<0.01$, $^{***}p<0.001$, two-tailed unpaired student *t*-test. F, G) Representative micrographs of neocortical or hippocampal sections showing the decrease in 6E10 plaque staining intensity as a consequence of ACI-91 treatment. Scale = 200 μm.

was injected in the striatum two hours after the last compound application, and $[^{125}I]A\beta_{1\text{-}40}$ activity determined in different tissues 40 min later. ACI-91 treatment significantly reduced $[^{125}I]A\beta_{1\text{-}40}$ in the injected brain hemisphere when compared to vehicle treated animals (Fig. 7A, −38%). Only traces of $[^{125}I]A\beta_{1\text{-}40}$ were detected in the contralateral hemibrain (Fig. 7B), confirming no spillover from the injected hemisphere, and no effect of ACI-91 was observed. ACI-91 treatment did not affect significantly CSF $[^{125}I]A\beta_{1\text{-}40}$ (Fig. 7C), suggesting that ACI-91 may act on the direct brain-to-blood efflux of Aβ without involving the drainage through the CSF. Interestingly, ACI-91 also reduced $[^{125}I]A\beta_{1\text{-}40}$ in blood (Fig. 7D, −40%) and liver (Fig. 7E, −38%) but not in kidney (Fig. 7F), possibly suggesting peripheral clearance of brain-derived Aβ through the kidneys. This was explored further in a study performed in non-transgenic $hA\beta PP_{SL}$ littermate mice whereby multiple tissues were analyzed 20 or 60 min after intrathecal injection (Table 2). At 20 min, 80% of the total activity was still present in the injected hemibrain, whereas the $[^{125}I]A\beta_{1\text{-}40}$ measured in the contralateral hemibrain was only slightly above the background values. At 60 min, the relative amount of $[^{125}I]A\beta_{1\text{-}40}$ in the injected brain hemispheres was reduced to 52% of the total activity with redistribution into most peripheral tissues. Between 20 and 60 min, $[^{125}I]A\beta_{1\text{-}40}$ increased in blood (+77%), liver (+103%), kidney (+59%), intestine (+157%), and heart (+83%). The largest relative increase (+780%) between the two time points as well as the largest relative amount at 60 min (15.8 ± 3.3%) were found in urine (Table 2), showing that $[^{125}I]A\beta_{1\text{-}40}$ excretion occurred through this route.

To study the role of passive and active brain efflux, in the next experiment we injected $[^{125}I]A\beta_{1\text{-}40}$ supple-

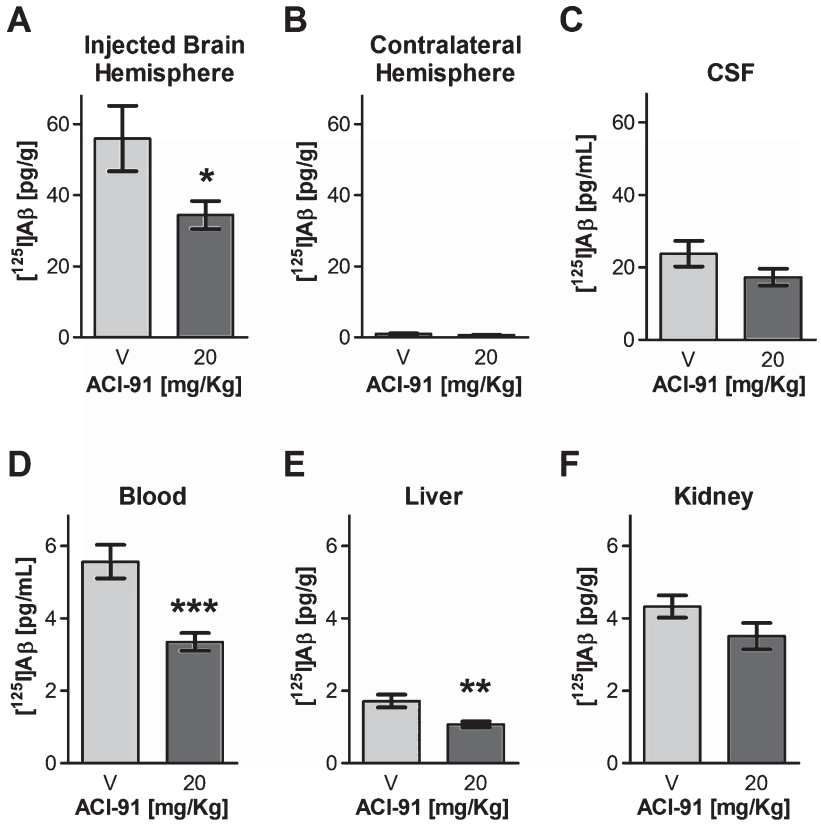

Fig. 7. Oral treatment with ACI-91 increases [^{125}I]Aβ clearance from brain and periphery. hAβPP$_{SL}$ mice at 9 months of age were treated for 33 days by daily gavage with vehicle (V, $n=9$) or 20 mg/Kg ACI-91 ($n=9$). Two hours after the last administration, 625 pg/g [^{125}I]Aβ$_{1\text{-}40}$ (1820 Ci/mmol) were intrathecally injected in the striatum. Residual [^{125}I]Aβ at 40 min after injection is significantly reduced for the ACI-91-treated animals in the injected brain hemisphere (A), blood (D), and liver (E) but not in the contralateral brain hemisphere (B), CSF (C), or kidney (F). All values are shown as average ± SEM. *$p<0.05$, **$p<0.01$, ***$p<0.001$, two-tailed unpaired student t-test.

Table 2
[^{125}]Aβ$_{1\text{-}40}$ radioactivity recovered 20 or 60 min after intrathecal injection in multiple tissues of non-transgenic hAβPP$_{SL}$ mice at 9 months of age. Data are reported as relative percent with respect to the total amount, average ± SEM, $n=8$-9, unpaired student t-test between the respective 20 and 60 min time points

	20 min	60 min	p	Change
Injected brain hemisphere	80.0 ± 2.4	51.6 ± 4.9	0.0008	−36
Contralateral hemisphere	1.4 ± 0.4	1.9 ± 0.3	0.34	ns
CSF	0.15 ± 0.04	0.32 ± 0.08	0.11	ns
Urine	1.8 ± 0.8	15.8 ± 3.3	0.003	+780
Blood	8.7 ± 1.1	15.4 ± 2.2	0.028	+77
Liver	3.1 ± 0.5	6.3 ± 1.0	0.018	+103
Kidney	2.4 ± 0.3	3.8 ± 0.3	0.010	+59
Intestine	1.0 ± 0.1	2.6 ± 0.3	0.0006	+157
Lung	1.1 ± 0.1	1.7 ± 0.2	0.057	ns
Heart	0.34 ± 0.04	0.63 ± 0.05	0.003	+83

ns, not significant.

mented with [^{14}C]inulin, which is a polar impermeable tracer with limited BBB permeability, thus a marker for passive transport [28, 43]. This allowed the normalization of the amount of [^{125}I]Aβ$_{1\text{-}40}$ with the amount of [^{14}C]inulin using the brain efflux index [43, 44]. For this study, we used hAβPP$_{SL}$ mice at an age of 9 months and treated daily for 37 days with vehicle or 20 mg/Kg ACI-91. Again, ACI-91 increased the clearance of [^{125}I]Aβ$_{1\text{-}40}$ from brain 20 min after intrathecal injection (63%) but not after 40 min (Fig. 8A), i.e., at the time point when the fast rate of [^{125}I]Aβ$_{1\text{-}40}$ brain clearance was completed also in the vehicle-treated animals (not shown). The amount of [^{125}I]Aβ$_{1\text{-}40}$ recovered in the contralateral hemisphere was low and the effect of ACI-91 did not reach significance (Fig. 8B). Consistent with rapid Aβ peripheral clearance, the reduction induced by ACI-91 at 20 min post-injection was also observed in blood (Fig. 8C, 69%) and stomach (Fig. 8D, 77%). The only significant effect observed at 60 min post-injection was found in urine, where ACI-91 treatment caused a robust [^{125}I]Aβ$_{1\text{-}40}$ increase resulting in a negative "clearance" value (Fig. 8E, −108%).

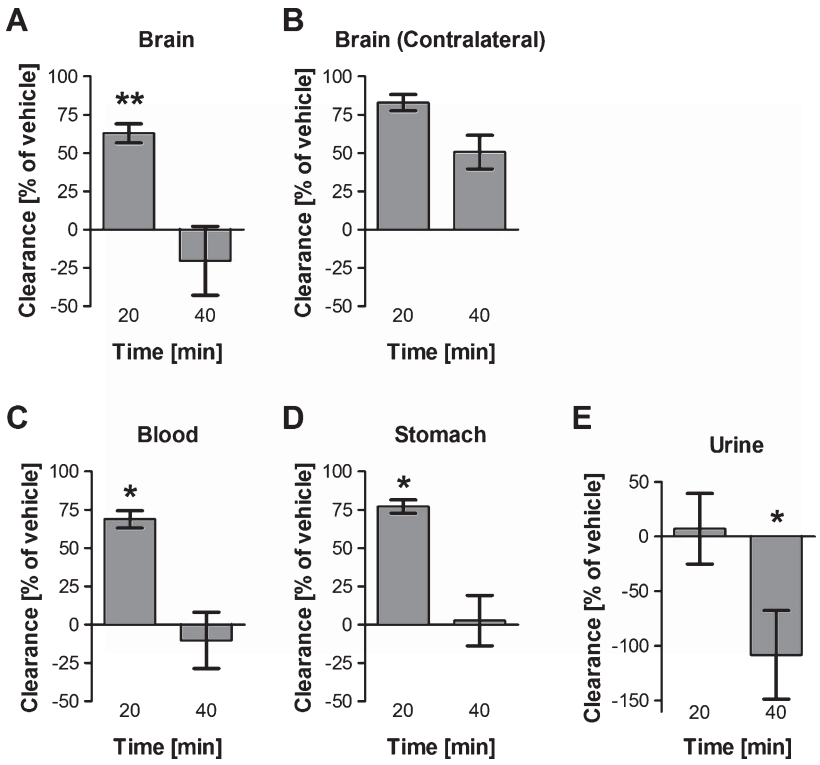

Fig. 8. Induced Aβ clearance by ACI-91 analyzed by the brain efflux index. hAβPP$_{SL}$ female mice at 9 months of age were treated for 37 days by daily gavage with vehicle or 20 mg/Kg ACI-91 ($n = 7$–9). Two hours after the last treatment, 625 pg/g [^{125}I]Aβ$_{1\text{-}40}$ (1820 Ci/mmol) and 2.8 μg/g [^{14}C]inulin (1.2 Ci/g) were injected in the striatum. Residual [^{125}I]Aβ was determined 20 and 40 min later and values normalized to residual brain [^{14}C]inulin and shown as percent of the respective vehicle values in the injected brain hemisphere (A), contralateral hemisphere (B), blood (C), stomach (D), and urine (E). All values are average ± SEM. *$p < 0.05$, **$p < 0.01$, two-tailed unpaired student t-test when comparing vehicle and ACI-91.

In order to assess the effect of ACI-91 on the homeostasis of Aβ in the ISF of the brain, we made use of *in vivo* microdialysis. This technique also allows to study drugs effects over time in awaken moving mice [31, 32]. A 38 kDa cut-off probe was implanted unilaterally in the hippocampus of mhAβPP/PS1d mice at 2-3 months of age. At this age, the mice have not yet developed Aβ pathology, enabling to study the effect of ACI-91 on Aβ metabolism without a possible interference of Aβ accumulation. After recovery from surgery, ISF was sampled hourly at a flow rate of 1 μl/min in order to determine basal ISF Aβ for intra-animal normalization. Following a single oral administration of 20 mg/Kg ACI-91 or vehicle, ISF was sampled for 24 h and Aβ determined by ELISA. Consistent with the pharmacokinetics of ACI-91, two-way ANOVA repeated analysis showed an effect of treatment and time with a 20–28% reduction of ISF Aβ in the ACI-91-treated mice between 5 and 9 h after compound administration when compared to the stable ISF Aβ levels in the vehicle-treated mice (Fig. 9A). ISF Aβ returned then to normal levels between 10 and 12 h post-treatment.

In order to determine the elimination half-life of ISF Aβ, mice were administered 24 h after initial dosing with vehicle or ACI-91. Just before start of the ACI-91 effect, all mice were treated with a γ-secretase inhibitor to block Aβ generation, which enabled assessing the elimination rate of ISF Aβ. The half-life of brain Aβ in the vehicle-treated mice was 1.54 ± 0.15 h, whereas Aβ in ACI-91-treated mice had a shorter half-life of 1.07 ± 0.06 h (Fig. 9B). This result is consistent with the increased brain efflux observed after intrathecal injection of labeled Aβ (Figs. 4–6).

ACI-91 modulates the mRNA levels of multiple transporters and tight junction proteins in brain microvessels and cultured endothelial cells

To assess whether the increase in Aβ brain efflux by ACI-91 treatment was caused by a direct effect on brain endothelial cells, brain microvessels were

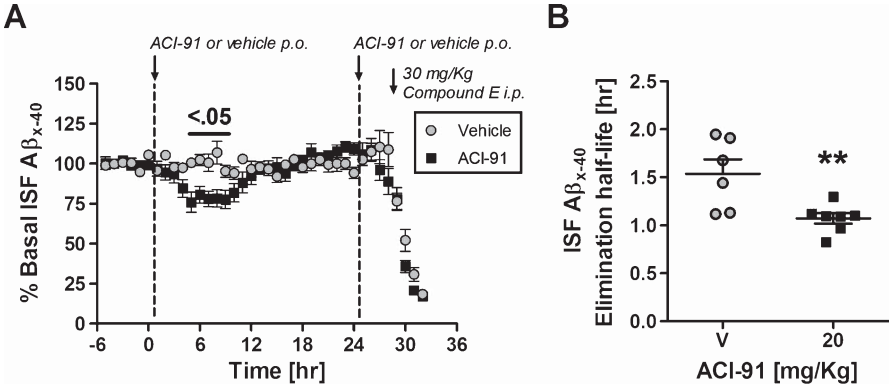

Fig. 9. Orally administered ACI-91 increases clearance of interstitial fluid Aβ. A) Interstitial fluid (ISF) human $A\beta_{x-40}$ was determined every hour by *in vivo* microdialysis in mhAβPP/PS1d mice at 2-3 months of age. Six hours after implanting the microdialysis in the hippocampus, the mice were given a single oral bolus of vehicle ($n=9$) or 20 mg/Kg ACI-91 ($n=10$). ISF $A\beta_{x-40}$ was significantly reduced between 5 and 9 h post-treatment (treatment $p=0.023$, time $p<0.0001$, and interaction $p<0.0001$, two-way ANOVA repeated measure and Bonferroni post-test analysis). B) Elimination half-life of ISF $A\beta_{x-40}$ was determined 24 h after initial dosing by repeating the same treatment with vehicle ($n=6$) or ACI-91 ($n=7$) followed 4 h later by i.p. administration of 30 mg/Kg Compound E, a γ-secretase inhibitor. Values are shown as average ± SEM. $^{**}p=0.01$, two-tailed unpaired student *t*-test.

isolated from nine month-old $hA\beta PP_{SL}$ mice treated for 33 days with 20 mg/Kg ACI-91 or vehicle and the isolated microvessels screened for changes in the expression of several genes known to be involved in BBB barrier function or Aβ transport across the BBB. A selection of transcripts was reevaluated in triplicate by real-time PCR analysis (Fig. 10A). The mRNA for several active efflux transporters were significantly increased in ACI-91 treated animals. Beside the LDL receptor (LDLR), the Aβ transporters LRP1 [14, 15, 28, 42] and P-glycoprotein [17], as well as apolipoprotein E (ApoE) were upregulated. Other MDR family members, MRP4 and ABCG2, were unchanged. In contrast, the mRNA encoding for the receptor for advanced glycation end-products (RAGE), a membrane protein that has been reported to mediate the transport of Aβ from the periphery into the brain [18], was down-regulated. Also reduced was the mRNA encoding for the muscarinic AChR M1. BBB markers such as the tight junction proteins claudin-5 and zona occludens protein 1, the endothelial basement membrane molecule laminin-5 as well as the glucose-transporter 1 (GLUT1), some of which are known to be down-regulated in AD [45, 46], were significantly upregulated with ACI treatment, possibly indicating a return to the normal BBB phenotype. There was however no difference in vascular endothelial cadherin 5 (VECad, CD144), in transporters such as the neonatal Fc receptor (FcRn) and the Na/K ATPase, or in the house-keeping gene RNA polymerase.

Expression analysis was also performed on primary MBMECs treated with ACI-91 (Fig. 10B). When cultured on filters, MBMECs form confluent, electrical resistant cell monolayers that retain certain barrier functions of the brain microvasculature [35]. Similar to the changes observed in the isolated brain microvessels, ACI-91 treatment induced upregulation of active transporters such as LRP1, LDLR, and P-glycoprotein. Also the mRNA for VLDLR and FcRn were increased in the ACI-91 treated MBMECs. In contrast, ApoE, RAGE, MRP4, ABCG2, and ABCC4 did not change and the same was observed for VECad, claudin-5, and GLUT1. These differences in expression between cultured cells and freshly isolated vessels might be a result of culture induced down-regulation as observed for ApoE (not shown) and reported previously for many BBB markers such as GLUT1 and claudin-5 [47]. Interestingly, the mRNA encoding for the muscarinic AChR M1, but not for M3, was also increased in the ACI-91-treated cells when compared to the control cells, which is consistent with the expected upregulation in receptor expression in the presence of a specific antagonist [48].

These data show a pharmacodynamic action of ACI-91 at the BBB. The changes in the expression of Aβ transporters observed in brain endothelial cells are consistent with the increased Aβ brain efflux observed following ACI-91 administration in different transgenic mouse lines (Figs. 6–9).

ACI-91 upregulates active transport through brain endothelial cells in vitro

MBMECs were used to show that LRP1 play a critical role for the active transport of Aβ *in vitro*

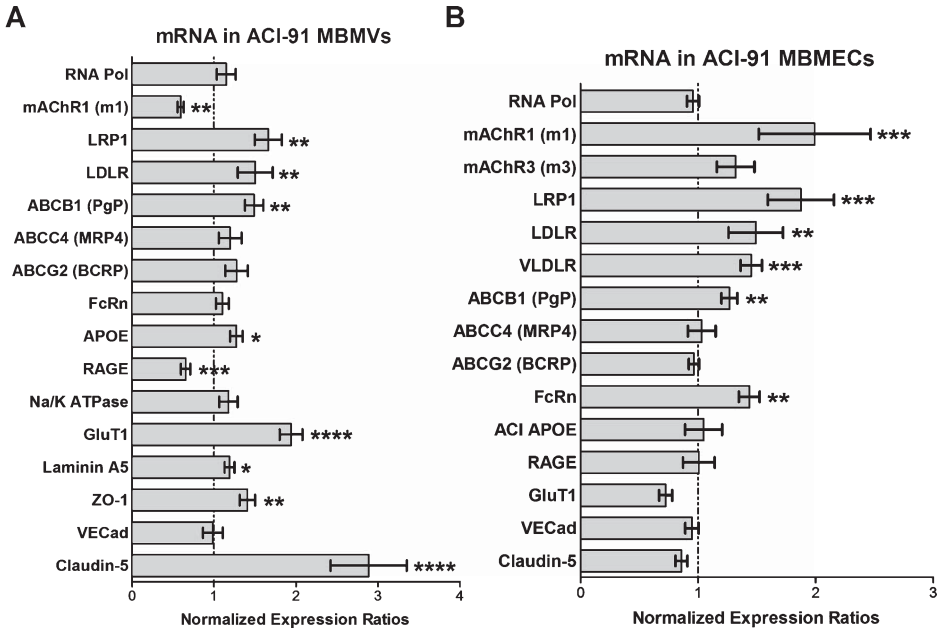

Fig. 10. ACI-91 changes expression of multiple mRNAs *in vivo* and *in vitro*. A) Triplicate qPCR analysis of multiple targets was performed *ex vivo* on total RNA prepared from brain microvessels (MBMVs) isolated from 10 month-old hAβPP$_{SL}$ mice treated for 33 days by daily gavage with vehicle ($n = 18$) or 20 mg/Kg ACI-91 ($n = 17$). For each mRNA, expression ($2^{-\Delta\Delta Ct}$) was normalized to the G6PDX mRNA. Values obtained for the ACI-91-treated animals are shown as ratio over control vehicle conditions (average ± SEM). B) mRNA expression analysis was also performed using total RNA isolated from differentiated primary mouse brain microvascular endothelial cells (MBMECs) treated for 24 h in the absence or presence of 10 μM ACI-91. *$p < 0.05$, **$p < 0.01$, ***$p < 0.001$, paired two-way ANOVA.

[49]. We first establish the Aβ transport assay using fluorescent DEAC-labeled Aβ$_{1\text{-}40}$ (active transport) and TxR-labeled 3 kDa dextran (passive transport), which served as internal control for the tightness of the MBMEC monolayer. The transport experiment was started by adding the two tracers to the medium of the top chamber of MBMEC monolayer culture. Medium samples were collected from the bottom chamber of the transwell insert after 10 min and analyzed to detect the presence of the fluorescent tracers. Under these conditions, the presence of a 10-fold excess of unlabeled Aβ inhibited DEAC-Aβ transport indicating an active, saturable transport mechanism of Aβ by MBMEC monolayers (Fig. 11A). In contrast, paracellular leakage of TxR-3 kDa dextran was low (not shown) and no effect of excess Aβ was observed (Fig. 11B), demonstrating a functional barrier by the MBMEC monolayers and no Aβ-mediated toxicity. When the cells were pre-incubated for 24 h with 10 μM ACI-91, Aβ$_{1\text{-}40}$ transport through the MBMEC monolayer was increased (Fig. 11C). These data are consistent with the increase in mRNA expression for abluminal Aβ transporters LRP-1, LDLR, and P-glycoprotein and down-regulation of the mRNA for the luminal transporter RAGE (Fig. 10). In contrast, the transport of dextran was not affected by the presence of ACI-91 (Fig. 11D), indicating no compound-related toxicity on the integrity of MBMEC monolayer. Indeed, the transendothelial electrical resistance of the MBMEC monolayer was not affected up to 140 μM ACI-91 ($97.4 \pm 3.7\%$; $20.82 + 0.51$ Ω.cm^2) compared to vehicle control ($100.0 \pm 0.4\%$; $21.69 + 2.98$ Ω.cm^2). These experiments were repeated using bEnd5 cells, which are an immortalized mouse brain endothelioma cell line well characterized as an *in vitro* BBB model [38]. Virtually the same results were obtained when bEnd5 cells, instead of the primary endothelial cells were used to prepare the *in vitro* BBB model (Fig. 11E, F).

Consistent with the action of ACI-91, the presence of 10 μM Darifenacin also increased Aβ transport over the bEnd5 cell monolayer (Fig. 11G, H). ACI-91 and Darifenacin are both similarly potent inhibitors of muscarinic receptors but the chemical structures of these two compounds are unrelated. We conclude that the effects of ACI-91 on Aβ efflux described in our studies are caused by its well-described property as selective negative allosteric modulators of muscarinic AChR rather than an unrelated, compound-specific mode of action.

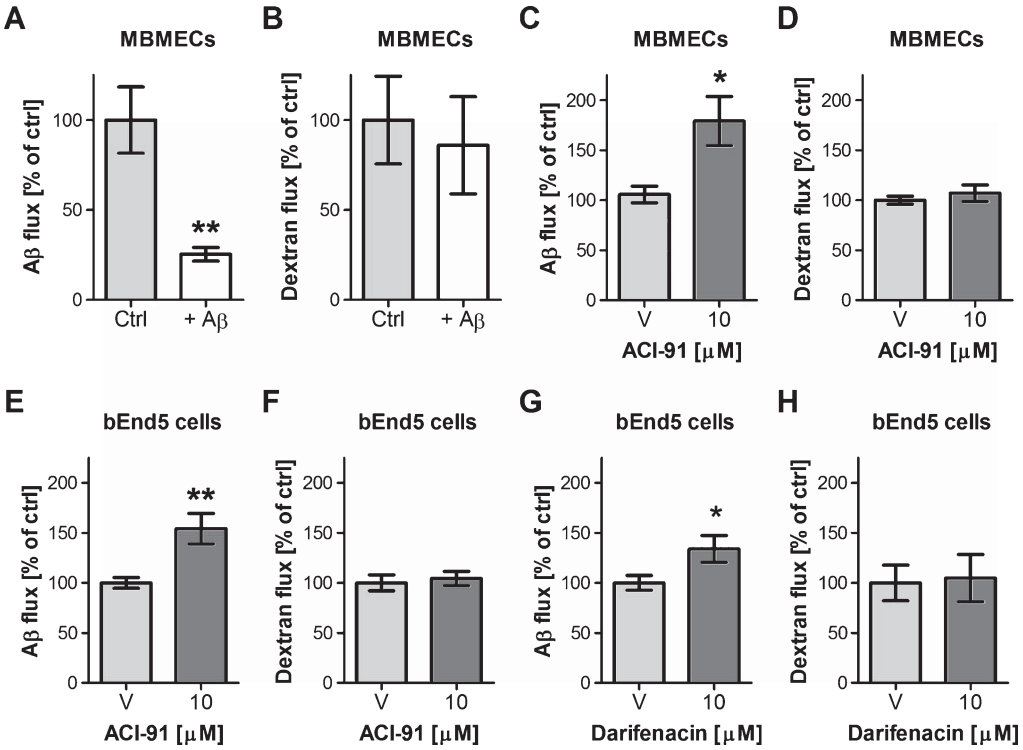

Fig. 11. mAChR antagonists increase active Aβ transport by differentiated endothelia cells *in vitro*. Primary mouse brain endothelial cells (MBMECs, A-D) or bEnd5 cells (E-F) were differentiated into a tight monolayer on filters, 1 μM DEAC-$A\beta_{1\text{-}40}$ and 5 μM TxR-3 kDa dextran were added as a mixture to the top chamber and 10 min later samples from the top and bottom chambers were collected and analyzed. Relative top to bottom chamber flux values are shown as average ± SEM for Aβ (DEAC-fluorescence) or for dextran (TxR-fluorescence) as percent of control conditions ($n = 4$ for A and B; $n = 6$ for C and D; $n = 10$ for E and F; $n = 8$ for G and H). A, B) Cell monolayers were incubated in the absence (Ctrl) or presence of 10-fold excess unlabeled $A\beta_{1\text{-}40}$. C-F) Cell monolayers were treated for 24 h preceding as well as during the transport experiment in the absence (V) or presence of ACI-91. *$p < 0.05$, **$p < 0.01$, two-tailed unpaired student *t*-test.

DISCUSSION

Aβ clearance deficits rather than increased Aβ production were reported to contribute to its accumulation in the AD brain [8]. Thus, pharmacological boosting of Aβ efflux through the BBB could represent an effective strategy to reduce brain Aβ [9]. We report that ACI-91, a negative allosteric modulator of muscarinic receptors, increases Aβ efflux from brain in AβPP transgenic mice. Notably, the site of action of ACI-91 appears located on endothelial cells of the BBB, suggesting that reduction of brain Aβ can be achieved without the need of a brain-penetrating drug. Increased Aβ efflux may have contributed to the reduction of Aβ deposition and to the amelioration of behavioral deficits in AβPP transgenic mice observed after ACI-91 treatment.

Increase in brain efflux of Aβ following ACI-91 treatment was shown in three different transgenic mouse models using three different technologies. Consistent with published data [28], [^{125}I]Aβ is rapidly cleared from brain with basal levels reached within the first hour after intrathecal application in the striatum, and we further confirmed this result using also biotin-Aβ. Daily ACI-91 treatment for 33 days accelerates brain efflux of [^{125}I]Aβ in 9 month-old $hA\beta PP_{SL}$ mice and of biotin-Aβ in 11 month-old AβPP/PS1 mice. The fact that Aβ efflux was increased in the presence of severe plaque burden indicates that ACI-91 is active also when Aβ recruitment into plaques competes against Aβ clearance, and possibly also in the presence of disease-related reduction of Aβ efflux as reported for AD [8]. In the third experimental model, *in vivo* microdialysis in young pre-plaque mhAβPP/PS1d mice demonstrates a faster brain Aβ half-life following a single ACI-91 administration.

The pharmacodynamic response obtained in the microdialysis study, i.e., transient reduction of ISF Aβ

between 5 and 9 h after oral administration of ACI-91, is consistent with the pharmacokinetics of ACI-91. Rat studies showed that oral administration of Pirenzepine (ACI-91) resulted in maximal plasma concentration at 3 h post-administration and full drug disposal at 24 h [50]. The pharmacodynamic study shows that ACI-91 also increases the clearance of brain-borne Aβ in blood and most peripheral tissues with the exception of kidney. The accumulation of Aβ in urine in ACI-91 treated mice indicates an augmented urinal excretion of Aβ when compared to the vehicle treated animals.

We did not formally exclude the contribution of a central effect of ACI-91 on Aβ accumulation, as it may be expected by the well-known contribution of muscarinic receptor on AβPP processing and Aβ formation [20, 21]. Also, it has been shown that Pirenzepine significantly impairs recognition memory after microinfusion into perirhinal cortex of monkey [51], disrupts short-term memory after intracerebroventricular administration in rats [52], and impairs spontaneous alternation performance after intracerebroventricular administration in mice [53]. Nevertheless, the increase of Aβ efflux observed in this study could fully explain the reduced Aβ accumulation observed after ACI-91 treatment in the mouse models of central AD-like amyloidosis. Neocortical plaque accumulation is reduced in AβPPPS1 mice treated orally with 100 mg/Kg ACI-91 between the fourth and fifth month of age and in $hA\beta PP_{SL}$ mice treated at six months. At 20 mg/Kg, ACI-91 reduces neocortical plaques in $hA\beta PP_{SL}$ mice and neocortical and hippocampal plaques in AβPP/PS1 mice. Overall, ACI-91 shows a clear dose-dependency as a daily 5 mg/Kg dose fails to produce a significant effect in any of the read-outs analyzed in this study.

Consistent with the reduced plaque pathology found by immune histology, biochemical analysis of brain homogenate fractions demonstrates a decrease in insoluble brain Aβ in $hA\beta PP_{SL}$ mice. ACI-91 treatment reduces the accumulation of both $A\beta_{x\text{-}40}$ and $A\beta_{x\text{-}42}$ peptides, suggesting that increased brain efflux by ACI-91 may embrace different Aβ peptides. Supporting this hypothesis, in $hA\beta PP_{SL}$ mice treated with ACI-91 we find reduced CSF levels accompanied by increased plasma levels for both peptides.

ACI-91 also alleviates behavioral deficits in plaque-bearing mice in terms of improved spatial memory in the water maze test. Behavioral deficits in the human AβPP transgenic mice have been suggested to be caused by oligomeric soluble species Aβ [54]. Although technical limitations did not allow for specific analysis of the effect of ACI-91 on brain Aβ oligomers, rescue of the behavioral deficits in the $hA\beta PP_{SL}$ mice was observed in parallel to a relatively small 14% reduction in plaque area and 22% reduction in plaque number. This supports the view that the main brain target of ACI-91 is the soluble Aβ pool. In AβPP/PS1 mice, plaque number and area are less profoundly affected than intensity of plaque staining with an Aβ antibody or Thioflavin S. This again suggests that ACI-91 treatment inhibits the recruitment of soluble Aβ species into existing plaques and thus their maturation into Thioflavin-positive dense-core plaques.

It is interesting to note that Pirenzepine displays poor brain penetration in several species including rodents [41]. Our bioavailability studies in mice confirmed this property of ACI-91. Therefore, the site of action of ACI-91 is likely to be outside the brain parenchyma, possibly at the luminal site of brain capillaries, which is supported by the changes in gene transcription observed in brain microvessels isolated from ACI-91 treated animals. From this, we postulate a cascade of events where Aβ efflux at the BBB is the primary effect of ACI-91 followed by improved spatial memory and inhibition of plaque pathology progression. Inhibition of muscarinic receptors restricted to the periphery may present a therapeutic advantage. In the brain, muscarinic agonists improve, whereas muscarinic antagonists exacerbate AD-like symptoms [55] and muscarinic agonists, rather than antagonists, are currently tested in clinical trials [56, 57].

Accelerated Aβ efflux by ACI-91 in mice was first studied after daily treatment for 33 days. The single bolus study performed by *in vivo* microdyalisis shows that the molecular changes at the BBB involved in this process occur rapidly. Also, these data show that increased Aβ transport by ACI-91 is not restricted to a reversal of disease-induced deficits in old mice. These observations encouraged us to extend our studies to more accessible *in vitro* cell systems. Using endothelial monolayers made either of primary MBMECs or bEnd5 cells, we show that active Aβ transport is augmented by a relatively short treatment with ACI-91 when compared to control conditions. Interestingly, the same effect is observed in the presence of the structurally unrelated inhibitor of muscarinic receptors Darifenacin [58], demonstrating that inhibition of muscarinic activity is the primary cause for the upregulation of Aβ transport.

Pirenzepine (ACI-91) shows preference for the M1/M4 subclasses with an affinity for these receptors 5–10-fold higher than for the M3 subclass [23]. In contrast, Darifenacin shows an opposite prefer-

ence with 4–15-fold higher affinity for the M3/M5 subclasses over the M1/M4 subclasses [59] and both drugs have relatively weak M2 affinities. Endothelial cells express all muscarinic AChR subtypes with the exception of M4 [60]. These data imply that ACI-91 and Darifenacin may inhibit M1/M3/M5 receptors resulting in increased Aβ efflux. While M2/M4 receptors are coupled to adenylate cyclase and modulate cAMP levels, M1/M3/M5 receptors are coupled to phospholipase C and ultimately increase cytosolic Ca^{2+} and activate PKC [23]. cAMP was shown to increase the barrier properties of bovine brain endothelial cells whereas PKC did the opposite [61]. Along with the modulation of paracellular permeability of endothelial cells by PKC [62], expression of transporter such as P-glycoprotein may increase [63], which was also observed in the current study and again supports an involvement of muscarinic receptors in Aβ efflux. In line with the role that muscarinic receptors may have in regulating endothelial cell function, we show that ACI-91 profoundly affects the expression of multiple endothelial cell genes involved in Aβ transport across the BBB (LDLR, LRP1, P-glycoprotein, ApoE, and RAGE). The mechanisms coupling muscarinic receptor inhibition with mRNA expression remain unclear at this point. Nevertheless, the upregulation of the transporters involved in Aβ efflux and down-regulation of the transporter that acts in the opposite direction, i.e., from the periphery to the brain, may explain the effect of ACI-91 on Aβ efflux at the murine BBB. Interestingly, smooth muscle cells of brain microvessels also express muscarinic receptors [60]. While M3 activation induces smooth muscle contraction, endothelial-dependent activation of M3 receptors causes relaxation of adjacent vascular smooth muscle cells via a nitric oxide-mediated effect [60]. This complex chain of events may explain the somehow contradictory observation that *in vivo* treatment with ACI-91 down-regulates the M1 mRNA in brain microvessels and has the inverse effect in cultured endothelial cells through a more classical antagonist-induced upregulation of a G protein-coupled receptor [48]. Finally, muscarinic receptors are also localized on perivascular astrocyte endfeet [64], and the contribution of an astrocytic pathway in Aβ efflux has been recently suggested [65]. Therefore, this mechanism cannot be excluded from contributing to the effects reported here.

The model that is supported best by our data is that M1/M3/M5 inhibition increases the transport capacity of Aβ by endothelial cells, thus decreasing Aβ burden in brain.

ACKNOWLEDGMENTS

We would like to thank the Phenotyping Unit EPFL/SV/UDP and reMYND for their technical support. KD and SL were supported by grants received by LS from the Deutsche Forschungsgemeinschaft (SFB/TR23 B7 Vascular Differentiation and Remodeling to SL, the LOEWE Initiative Hessen (Oncogenic Signal Transduction Frankfurt, III L 4-518/55.004, 2009) and the Excellence Cluster Cardio-Pulmonary System. BP was supported by the EC FP-7 Health project No. 201159 "Memoload".

Authors' disclosures available online (http://www.j-alz.com/disclosures/view.php?id=1902).

REFERENCES

[1] Palop JJ, Mucke L (2010) Amyloid-beta-induced neuronal dysfunction in Alzheimer's disease: From synapses toward neural networks. *Nat Neurosci* **13**, 812-818.

[2] Benilova I, Karran E, De Strooper B (2012) The toxic Aβ oligomer and Alzheimer's disease: An emperor in need of clothes. *Nat Neurosci* **15**, 349-357.

[3] Huang Y, Mucke L (2012) Alzheimer mechanisms and therapeutic strategies. *Cell* **148**, 1204-1222.

[4] O'Brien RJ, Wong PC (2011) Amyloid precursor protein processing and Alzheimer's disease. *Annu Rev Neurosci* **34**, 185-204.

[5] Bertram L, Tanzi RE (2012) The genetics of Alzheimer's disease. *Prog Mol Biol Transl Sci* **107**, 79-100.

[6] Kitazawa M, Medeiros R, Laferla FM (2012) Transgenic mouse models of Alzheimer disease: Developing a better model as a tool for therapeutic interventions. *Curr Pharm Des* **18**, 1131-1147.

[7] Citron M (2010) Alzheimer's disease: Strategies for disease modification. *Nat Rev Drug Discov* **9**, 387-398.

[8] Mawuenyega KG, Sigurdson W, Ovod V, Munsell L, Kasten T, Morris JC, Yarasheski KE, Bateman RJ (2010) Decreased clearance of CNS beta-amyloid in Alzheimer's disease. *Science* **330**, 1774.

[9] Kurz A, Perneczky RJ (2011) Amyloid clearance as a treatment target against Alzheimer's disease. *J Alzheimers Dis* **24** (Suppl 2), 61-73.

[10] Sagare AP, Bell RD, Zlokovic BV (2012) Neurovascular dysfunction and faulty amyloid β-peptide clearance in Alzheimer disease. *Cold Spring Harb Perspect Med* **2**, pii:a011452.

[11] Zlokovic BV (2004) Clearing amyloid through the blood-brain barrier. *J Neurochem* **89**, 807-811.

[12] Van Uden E, Mallory M, Veinbergs I, Alford M, Rockenstein E, Masliah E (2002) Increased extracellular amyloid deposition and neurodegeneration in human amyloid precursor protein transgenic mice deficient in receptor-associated protein. *J Neurosci* **22**, 9298-9304.

[13] Xu G, Karch C, Li N, Lin N, Fromholt D, Gonzales V, Borchelt DR (2008) Receptor-associated protein (RAP) plays a central role in modulating Abeta deposition in APP/PS1 transgenic mice. *PLoS One* **3**, e3159.

[14] Jaeger LB, Dohgu S, Hwang MC, Farr SA, Murphy MP, Fleegal-Demotta MA, Lynch JL, Robinson SM, Niehoff ML, Johnson SN, Kumar VB, Banks WA (2009) Testing the neurovascular hypothesis of Alzheimer's disease: LRP-

1 antisense reduces blood-brain barrier clearance, increases brain levels of amyloid-beta protein, and impairs cognition. *J Alzheimers Dis* **17**, 553-570.

[15] Kang DE, Pietrzik CU, Baum L, Chevallier N, Merriam DE, Kounnas MZ, Wagner SL, Troncoso JC, Kawas CH, Katzman R, Koo EH (2000) Modulation of amyloid beta-protein clearance and Alzheimer's disease susceptibility by the LDL receptor-related protein pathway. *J Clin Invest* **106**, 1159-1166.

[16] Tanzi RE, Moir RD, Wagner SL (2004) Clearance of Alzheimer's Abeta peptide: The many roads to perdition. *Neuron* **43**, 605-608.

[17] Cirrito JR, Deane R, Fagan AM, Spinner ML, Parsadanian M, Finn MB, Jiang H, Prior JL, Sagare A, Bales KR, Paul SM, Zlokovic BV, Piwnica-Worms D, Holtzman DM (2005) P-glycoprotein deficiency at the blood-brain barrier increases amyloid-beta deposition in an Alzheimer disease mouse model. *J Clin Invest* **115**, 3285-3290.

[18] Deane RJ (2012) Is RAGE still a therapeutic target for Alzheimer's disease? *Future Med Chem* **4**, 915-925.

[19] Sehgal N, Gupta A, Valli RK, Joshi SD, Mills JT, Hamel E, Khanna P, Jain SC, Thakur SS, Ravindranath V (2012) Withania somnifera reverses Alzheimer's disease pathology by enhancing low-density lipoprotein receptor related protein in liver. *Proc Natl Acad Sci U S A* **109**, 3510-3515.

[20] Hock C, Maddalena A, Raschig A, Müller-Spahn F, Eschweiler G, Hager K, Heuser I, Hampel H, Müller-Thomsen T, Oertel W, Wienrich M, Signorell A, Gonzalez-Agosti C, Nitsch RM (2003) Treatment with the selective muscarinic m1 agonist talsaclidine decreases cerebrospinal fluid levels of A beta 42 in patients with Alzheimer's disease. *Amyloid* **10**, 1-6.

[21] Fisher A (2012) Cholinergic modulation of amyloid precursor protein processing with emphasis on M1 muscarinic receptor: Perspectives and challenges in treatment of Alzheimer's disease. *J Neurochem* **120** (Suppl 1), 22-33.

[22] Kenakin T, Boselli C (1989) Pharmacologic discrimination between receptor heterogeneity and allosteric interaction: Resultant analysis of gallamine and pirenzepine antagonism of muscarinic responses in rat trachea. *J Pharmacol Exp Ther* **250**, 944-952.

[23] Caulfield MP, Birdsall NJ (1998) Classification of muscarinic acetylcholine receptors. *Pharmacol Rev* **50**, 279-290.

[24] Radde R, Bolmont T, Kaeser SA, Coomaraswamy J, Lindau D, Stoltze L, Calhoun ME, Jäggi F, Wolburg H, Gengler S, Haass C, Ghetti B, Czech C, Hölscher C, Mathews PM, Jucker M (2006) Abeta42-driven cerebral amyloidosis in transgenic mice reveals early and robust pathology. *EMBO Rep* **7**, 940-946.

[25] Rockenstein E, Mallory M, Mante M, Sisk A, Masliah E (2001) Early formation of mature amyloid-beta protein deposits in a mutant APP transgenic model depends on levels of Abeta(1-42). *J Neurosci Res* **66**, 573-582.

[26] Kawarabayashi T, Younkin LH, Saido TC, Shoji M, Ashe KH, Younkin SG (2001) Age-dependent changes in brain, CSF, and plasma amyloid (beta) protein in the Tg2576 transgenic mouse model of Alzheimer's disease. *J Neurosci* **21**, 372-381.

[27] Dewachter I, Van Dorpe J, Smeijers L, Gilis M, Kuipéri C, Laenen I, Caluwaerts N, Moechars D, Checler F, Vanderstichele H, Van Leuven F (2000) Aging increased amyloid peptide and caused amyloid plaques in brain of old APP/V717I transgenic mice by a different mechanism than mutant presenilin1. *J Neurosci* **20**, 6452-6458.

[28] Shibata M, Yamada S, Kumar SR, Calero M, Bading J, Frangione B, Holtzman DM, Miller CA, Strickland DK, Ghiso J, Zlokovic BV (2000) Clearance of Alzheimer's amyloid-ss(1-40) peptide from brain by LDL receptor-related protein-1 at the blood-brain barrier. *J Clin Invest* **106**, 1489-1499.

[29] Cui M, Ono M, Kimura H, Kawashima H, Liu BL, Saji H (2011) Radioiodinated benzimidazole derivatives as single photon emission computed tomography probes for imaging of β-amyloid plaques in Alzheimer's disease. *Nucl Med Biol* **38**, 313-320.

[30] Jankowsky JL, Slunt HH, Ratovitski T, Jenkins NA, Copeland NG, Borchelt DR (2001) Co-expression of multiple transgenes in mouse CNS: A comparison of strategies. *Biomol Eng* **17**, 157-165.

[31] Cirrito JR, May PC, O'Dell MA, Taylor JW, Parsadanian M, Cramer JW, Audia JE, Nissen JS, Bales KR, Paul SM, DeMattos RB, Holtzman DM (2003) *In vivo* assessment of brain interstitial fluid with microdialysis reveals plaque-associated changes in amyloid-beta metabolism and half-life. *J Neurosci* **23**, 8844-8853.

[32] Verges DK, Restivo JL, Goebel WD, Holtzman DM, Cirrito JR (2011) Opposing synaptic regulation of amyloid-beta metabolism by NMDA receptors *in vivo*. *J Neurosci* **31**, 11328-11337.

[33] Seiffert D, Bradley JD, Rominger CM, Rominger DH, Yang F, Meredith JE, Jr., Wang Q, Roach AH, Thompson LA, Spitz SM, Higaki JN, Prakash SR, Combs AP, Copeland RA, Arneric SP, Hartig PR, Robertson DW, Cordell B, Stern AM, Olson RE, Zaczek R (2000) Presenilin-1 and -2 are molecular targets for gamma-secretase inhibitors. *J Biol Chem* **275**, 34086-34091.

[34] Hong S, Quintero-Monzon O, Ostaszewski BL, Podlisny DR, Cavanaugh WT, Yang T, Holtzman DM, Cirrito JR, Selkoe DJ (2011) Dynamic analysis of amyloid β-protein in behaving mice reveals opposing changes in ISF versus parenchymal Aβ during age-related plaque formation. *J Neurosci* **31**, 15861-15869.

[35] Liebner S, Corada M, Bangsow T, Babbage J, Taddei A, Czupalla CJ, Reis M, Felici A, Wolburg H, Fruttiger M, Taketo MM, von Melchner H, Plate KH, Gerhardt H, Dejana E (2008) Wnt/beta-catenin signaling controls development of the blood-brain barrier. *J Cell Biol* **183**, 409-417.

[36] Fisher J, Devraj K, Ingram J, Slagle-Webb B, Madhankumar AB, Liu X, Klinger M, Simpson IA, Connor JR (2007) Ferritin: A novel mechanism for delivery of iron to the brain and other organs. *Am J Physiol Cell Physiol* **293**, C641-649.

[37] Paolinelli R, Corada M, Devraj K, Ferrarini L, Artus C, Czupalla C, Rudini N, Luigi M, Engelhardt B, Couraud PO, Liebner S, Dejana E (2013) Wnt activation of immortalized brain endothelial cells as a tool for generating a standardized model of the blood-brain barrier *in vitro*. *PLoS ONE* **8**, e70233.

[38] Reiss Y, Hoch G, Deutsch U, Engelhardt B (1998) T cell interaction with ICAM-1-deficient endothelium *in vitro*: Essential role for ICAM-1 and ICAM-2 in transendothelial migration of T cells. *Eur J Immunol* **28**, 3086-3099.

[39] Reis M, Czupalla CJ, Ziegler N, Devraj K, Zinke J, Seidel S, Heck R, Thom S, Macas J, Bockamp E, Fruttiger M, Taketo MM, Dimmeler S, Plate KH, Liebner S (2012) Endothelial Wnt/β-catenin signaling inhibits glioma angiogenesis and normalizes tumor blood vessels by inducing PDGF-B expression. *J Exp Med* **209**, 1611-1627.

[40] Abramowski D, Rabe S, Upadhaya AR, Reichwald J, Danner S, Staab D, Capetillo-Zarate E, Yamaguchi H, Saido TC, Wiederhold KH, Thal DR, Staufenbiel M (2012) Transgenic expression of intraneuronal Aβ42 but not Aβ40 leads to cellular Aβ lesions, degeneration, and functional impairment

without typical Alzheimer's disease pathology. *J Neurosci* **32**, 1273-1283.

[41] Carmine AA and Brogden RN (1985) Pirenzepine. A review of its pharmacodynamic and pharmacokinetic properties and therapeutic efficacy in peptic ulcer disease and other allied diseases. *Drugs* **30**, 85-126.

[42] Deane R, Wu Z, Sagare A, Davis J, Du Yan S, Hamm K, Xu F, Parisi M, LaRue B, Hu HW, Spijkers P, Guo H, Song X, Lenting PJ, Van Nostrand WE, Zlokovic BV (2004) LRP/amyloid beta-peptide interaction mediates differential brain efflux of Abeta isoforms. *Neuron* **43**, 333-344.

[43] Kakee A, Terasaki T, Sugiyama Y (1996) Brain efflux index as a novel method of analyzing efflux transport at the blood-brain barrier. *J Pharmacol Exp Ther* **227**, 1550-1559.

[44] Kusuhara H, Terasaki T, Sugiyama Y (2003) Brain efflux index method. Characterization of efflux transport across the blood-brain barrier. *Methods Mol Med* **89**, 219-231.

[45] Simpson IA, Chundu KR, Davies-Hill T, Honer WG, Davies P (1994) Decreased concentrations of GLUT1 and GLUT3 glucose transporters in the brains of patients with Alzheimer's disease. *Ann Neurol* **35**, 546-551.

[46] Hartz AM, Bauer B, Soldner EL, Wolf A, Boy S, Backhaus R, Mihaljevic I, Bogdahn U, Klünemann HH, Schuierer G, Schlachetzki F (2012) Amyloid-β contributes to blood-brain barrier leakage in transgenic human amyloid precursor protein mice and in humans with cerebral amyloid angiopathy. *Stroke* **43**, 514-523.

[47] Lyck R, Ruderisch N, Moll AG, Steiner O, Cohen CD, Engelhardt B, Makrides V, Verrey F (2009) Culture-induced changes in blood-brain barrier transcriptome: Implications for amino-acid transporters *in vivo*. *J Cereb Blood Flow Metab* **29**, 1491-1502.

[48] Fukamauchi F, Saunders PA, Hough C, Chuang DM (1993) Agonist-induced down-regulation and antagonist-induced up-regulation of m2- and m3-muscarinic acetylcholine receptor mRNA and protein in cultured cerebellar granule cells. *Mol Pharmacol* **44**, 940-949.

[49] Yamada K, Hashimoto T, Yabuki C, Nagae Y, Tachikawa M, Strickland DK, Liu Q, Bu G, Basak JM, Holtzman DM, Ohtsuki S, Terasaki T, Iwatsubo (2008) The low density lipoprotein receptor-related protein 1 mediates uptake of amyloid beta peptides in an *in vitro* model of the blood-brain barrier cells. *J Biol Chem* **283**, 34554-34562.

[50] Kobayashi S, Kyui S, Yoshida T, Nagakura A, Oiwa Y, Matsumura R, Kohei H (1981) Absorption, distribution and excretion of 14C-pirenzepine in rats. Accumulation characteristics after multiple dose regimen. *Arzneimittelforschung* **31**, 679-690.

[51] Wu W, Saunders RC, Mishkin M, Turchi J (2012) Differential effects of m1 and m2 receptor antagonists in perirhinal cortex on visual recognition memory in monkeys. *Neurobiol Learn Mem* **98**, 41-46.

[52] Aura J, Sirviö J, Riekkinen P Jr. (1997) Methoctramine moderately improves memory but pirenzepine disrupts performance in delayed non-matching to position test. *Eur J Pharmacol* **333**, 129-134.

[53] Ukai M, Shinkai N, Kameyama T (1995) Cholinergic receptor agonists inhibit Pirenzepine-induced dysfunction of spontaneous alternation performance in the mouse. *Gen Pharmacol* **26**, 1529-1532.

[54] Kittelberger KA, Piazza F, Tesco G, Reijmers LG (2012) Natural amyloid-beta oligomers acutely impair the formation of a contextual fear memory in mice. *PLoS One* **7**, e29940.

[55] Bubser M, Byun N, Wood MR, Jones CK (2012) Muscarinic receptor pharmacology and circuitry for the modulation of cognition. *Handb Exp Pharmacol* **208**, 121-166.

[56] Potter PE (2010) Investigational medications for treatment of patients with Alzheimer disease. *J Am Osteopath Assoc* **110**, S27-S36.

[57] Caccamo A, Fisher A, LaFerla FM (2009) M1 agonists as a potential disease-modifying therapy for Alzheimer's disease. *Curr Alzheimer Res* **6**, 112-117.

[58] Haab F (2005) Darifenacin for the treatment of overactive bladder. *Womens Health* **1**, 331-343.

[59] Ohtake A, Saitoh C, Yuyama H, Ukai M, Okutsu H, Noguchi Y, Hatanaka T, Suzuki M, Sato S, Sasamata M, Miyata K (2007) Pharmacological characterization of a new antimuscarinic agent, solifenacin succinate, in comparison with other antimuscarinic agents. *Biol Pharm Bull* **30**, 54-58.

[60] Elhusseiny A, Cohen Z, Olivier A, Stanimirović DB, Hamel E (1999) Functional acetylcholine muscarinic receptor subtypes in human brain microcirculation: Identification and cellular localization. *J Cereb Blood Flow Metab* **19**, 794-802.

[61] Rubin LL, Hall DE, Porter S, Barbu K, Cannon C, Horner HC, Janatpour M, Liaw CW, Manning K, Morales J, Tanner LI, Tomaselli KJ and Bard F (1991) A cell culture model of the blood-brain barrier. *J Cell Biol* **115**, 1725-17235.

[62] Willis CL, Meske DS, Davis TP (2010) Protein kinase C activation modulates reversible increase in cortical blood-brain barrier permeability and tight junction protein expression during hypoxia and posthypoxic reoxygenation. *J Cereb Blood Flow Metab* **30**, 1847-1859.

[63] Rigor RR, Hawkins BT, Miller DS (2010) Activation of PKC isoform beta(I) at the blood-brain barrier rapidly decreases P-glycoprotein activity and enhances drug delivery to the brain. *J Cereb Blood Flow Metab* **30**, 1373-1383.

[64] Moro V, Kacem K, Springhetti V, Seylaz J, Lasbennes F (1995) Microvessels isolated from brain: Localization of muscarinic sites by radioligand binding and immunofluorescent techniques. *J Cereb Blood Flow Metab* **15**, 1082-1092.

[65] Iliff JJ, Wang M, Liao Y, Plogg BA, Peng W, Gundersen GA, Benveniste H, Vates GE, Deane R, Goldman SA, Nagelhus EA, Nedergaard N (2012) A paravascular pathway facilitates CSF flow through the brain parenchyma and the clearance of interstitial solutes, including Amyloid β. *Sci Transl Med* **4**, 147ra111.